© 2015. Published by The Company of Biologists Ltd | Development (2015) 142, 4253-4265 doi:10.1242/dev.121020

New markers for tracking endoderm induction and hepatocyte differentiation from human pluripotent stem cells

Audrey Holtzinger[1], Philip R. Streeter[2], Farida Sarangi[1], Scott Hillborn[1], Maryam Niapour[1], Shinichiro Ogawa[1] and Gordon Keller[1,3,4,*]

ABSTRACT

The efficient generation of hepatocytes from human pluripotent stem cells (hPSCs) requires the induction of a proper endoderm population, broadly characterized by the expression of the cell surface marker CXCR4. Strategies to identify and isolate endoderm subpopulations predisposed to the liver fate do not exist. In this study, we generated mouse monoclonal antibodies against human embryonic stem cell-derived definitive endoderm with the goal of identifying cell surface markers that can be used to track the development of this germ layer and its specification to a hepatic fate. Through this approach, we identified two endoderm-specific antibodies, HDE1 and HDE2, which stain different stages of endoderm development and distinct derivative cell types. HDE1 marks a definitive endoderm population with high hepatic potential, whereas staining of HDE2 tracks with developing hepatocyte progenitors and hepatocytes. When used in combination, the staining patterns of these antibodies enable one to optimize endoderm induction and hepatic specification from any hPSC line.

KEY WORDS: Human pluripotent stem cell, Endoderm marker, Hepatocyte differentiation

INTRODUCTION

Human pluripotent stem cells (hPSCs), including both embryonic (hESCs) and induced pluripotent stem cells (hiPSCs), represent an unlimited source of differentiated cell types and tissues for modeling human development and disease *in vitro*, for developing new cell-based therapeutics and for establishing new drug discovery and predictive toxicology platforms (Cherry and Daley, 2012; Diecke et al., 2014; Fox et al., 2014; Holmgren et al., 2014; Leung et al., 2013; Medine et al., 2013; Roelandt et al., 2013; Sjogren et al., 2014; Szkolnicka et al., 2014; Trounson et al., 2012; Zhou et al., 2014). Translating this potential of stem cells into practice is, however, dependent on the availability of directed differentiation strategies that enable the efficient, reproducible and cost-effective generation of the lineage of interest. Of the different cell types that can be generated from hPSCs, substantial effort in recent years has been directed at the generation of endoderm-derived lineages, specifically pancreatic β-cells for transplantation for the treatment of type 1 diabetes and hepatocytes for predictive toxicology and drug metabolism studies (Holditch et al., 2014; Sun et al., 2013). This effort has led to advances in our basic understanding of human development and the generation of protocols for directed differentiation of hPSCs to pancreatic and hepatic fates that yield what seem to be highly enriched end-stage populations (Chen et al., 2012; Ogawa et al., 2013; Pagliuca et al., 2014; Rezania et al., 2014; Si-Tayeb et al., 2010). Despite this progress, efficiencies of differentiation vary considerably between different hPSC lines (Toivonen et al., 2013b; Vitale et al., 2012), even with the most advanced protocols, and end-stage populations are immature and, in some instances, contaminated with other cell types.

The first step in the derivation of pancreatic and hepatic lineage cells from hPSCs is the induction of definitive endoderm. Suboptimal endoderm induction is one likely cause of cell line-to-cell line and experiment-to-experiment variability because the non-endoderm cell types that differentiate in these conditions can influence pancreatic and hepatic differentiation and contribute to the development of heterogeneous end-stage populations. The efficiency of endoderm induction is monitored through changes in gene expression patterns and/or changes in the expression of surface markers as assessed by flow cytometry (D'Amour et al., 2005). The latter approach provides a rapid quantitative read-out but is dependent on the availability of antibodies against surface markers that should ideally be found only on the cells of interest. Currently, the markers most commonly used for monitoring endoderm induction from hPSCs are CD184 (CXCR4), CD117 (KIT) and EPCAM (D'Amour et al., 2005; Green et al., 2011; Jiang et al., 2013; Loh et al., 2014; Nostro et al., 2011; Ogawa et al., 2013). When used in combination, they do provide a reasonable assessment of the efficiency of endoderm development. However, as none of these markers is endoderm specific (Kataoka et al., 1997; McGrath et al., 1999; Sherwood et al., 2007; Witte, 1990), expression patterns can be misleading. The list of markers that can be used to monitor endoderm development has recently been extended to include CD49e (ITGA5) and CD51 (ITGAV) at the stage of definitive endoderm induction and CD141 (THBD) and CD238 (KEL) at the stage of patterning of the endoderm to a primitive gut tube stage (Brafman et al., 2013; Wang et al., 2011). As with the above markers, these are also not specific to the endoderm lineage. Currently, there are no known endoderm-specific cell surface markers that can be used to monitor endoderm induction or to isolate definitive endoderm populations from hPSC differentiation cultures.

To address this issue, we generated two monoclonal antibodies, HDE1 and HDE2, which specifically recognize hPSC-derived definitive endoderm. These antibodies show strikingly different patterns. HDE1 broadly stains the entire endoderm population and is induced from all hPSC lines tested. By contrast, HDE2 stains only a subpopulation of the early endoderm that can vary in size between different hPSC lines. By monitoring HDE1 staining at different times after activin induction, we show that the extent of staining is

[1]McEwen Centre for Regenerative Medicine, University Health Network, Toronto, Ontario, Canada M5G 1L7. [2]Oregon Stem Cell Center, Oregon Health & Science University, Portland, OR 97239-3098, USA. [3]Department of Medical Biophysics, University of Toronto, Toronto, Ontario, Canada M5G 2M9. [4]Princess Margaret Cancer Centre, Toronto, Ontario, Canada M5T 2M9.

*Author for correspondence (gkeller@uhnresearch.ca)

Received 12 December 2014; Accepted 13 October 2015

Development (2015) 142, 4253-4265 doi:10.1242/dev.121020

correlated with endoderm potential and that populations that are uniformly HDE1$^+$ are most efficient at generating hepatic progeny. After pancreatic and hepatic lineage specification, the patterns of HDE1 and HDE2 diverge, as HDE1 stains the non-endocrine cells in the pancreatic population but no hepatic cells, whereas HDE2 does not stain pancreatic lineage cells, with the exception of a few ductal cells, but does stain the emerging hepatic cells following specification. With these staining patterns, it is now possible to monitor both the endoderm induction and hepatic specification steps, enabling the optimization of hepatic differentiation from any hPSC line.

RESULTS

HDE1 and HDE2 are specific for hESC-derived definitive endoderm

To generate endoderm-specific antibodies, we used a strategy similar to the one we used to generate antibodies to mouse ESC-derived endoderm (Gadue et al., 2009). Here, BALB/c mice were immunized with HES2 hESC-derived definitive endoderm using standard polyethylene-mediated fusion technology (Köhler and Milstein, 1975). Supernatants from 800 successfully fused clones were originally screened for cell surface reactivity with hESC-derived definitive endoderm by flow cytometry. The endoderm population used for immunization was generated by inducing hESCs as embryoid bodies (EBs) with high concentrations of activin A for 4 days (from day 1 to 5). More than 95% of the induced population coexpressed the surface markers CXCR4, CD117 and EPCAM, and more than 90% of the cells expressed the endoderm transcription factor SOX17 as determined by intracellular flow cytometry (Fig. 1A). The purity of the population was documented further by the lack of contaminating KDR$^+$PDGFRα$^+$ mesodermal cells (Fig. 1A). We previously demonstrated that this endoderm population displays both pancreatic and hepatic potential (Nostro et al., 2011; Ogawa et al., 2013).

The resulting antibodies were initially screened for their ability to recognize the day 5 endoderm population and subsequently for a lack of reactivity with hESCs and hESC-derived mesoderm and neuroectoderm. With this strategy, we identified two antibodies, HDE1 and HDE2, which displayed interesting staining patterns. Both antibodies stained a subset of the day 5 CXCR4$^+$ endoderm population (Fig. 1B). By contrast, the vast majority of cells in the undifferentiated hESC population (Fig. 1C) and in the day 5 PDG FRα$^+$ cardiac mesoderm, the day 3 KDR$^+$CD56$^+$ hematopoietic mesoderm (Fig. 1D,E) and the day 7 KDR$^-$PDGFRα$^-$CD117$^-$ neuroectoderm (Fig. 1F) populations did not stain with either antibody. The small number of HDE1$^+$ cells detected in the meso derm populations is likely to reflect low levels of contaminating CXCR4$^+$CD117$^+$ endoderm. Cardiac mesoderm-derived populatio ns including the stages containing specified progenitors (days 8-12) and contracting cardiomyocytes (day 12-17) also did not stain with either antibody (data not shown). We next analyzed hESC-derived parietal-like endoderm to determine whether the HDE1 and HDE2 staining patterns would distinguish definitive and extra-embryonic endoderm. Parietal-like endoderm was generated using the protocol of Feng et al. (2012) and characterized as a COL4A1$^+$ population that expresses *SOX17*, *LAMB1*, *SPARC*, *THBD* and *SOX7* as described (Fig. 1G). HDE1 stained a small subpopulation of these cells, whereas none was positive for HDE2. Collectively, these findings demonstrate that both HDE1 and HDE2 show specificity fo r definitive endoderm at early stages of hESC differentiation.

Kinetic analyses of HES2-derived endoderm induction showed that low numbers of HDE1$^+$ cells were detected within 2 days of differentiation. The proportion of positive cells increased dramatically over the next 24 h and continued to increase to represent almost 90% of the entire population by day 5 of differentiation (Fig. 2A,B). This pattern is similar to that observed for the upregulation of SOX17 expression. CXCR4$^+$CD117$^+$ cells emerged rapidly, between days 2 and 3 of differentiation, and by day 4 more than 95% of the population expressed these markers (Fig. 2A,B). In contrast to the pattern of HDE1, relatively few cells stained with HDE2 during the first 4 days of differentiation. At day 5, a small HDE2$^+$ population was detected (Fig. 2A-C). The patterns for HDE1 staining were similar for H1 hESC-derived cells, although the proportion of positive cells at day 5 was lower than observed in the HES2-derived populations (Fig. 2C). Additionally, we observed the development of a transient population of HDE2$^+$ cells at day 3 of differentiation that was not detected in the HES2-derived cultures. Together, these findings show that the HDE1$^+$ cells develop in the EBs over a 5 day differentiation period, consistent with the emergence of definitive endoderm as measured by expression of the transcription factor SOX17 and by the surface markers CXCR4 and CD117. The observation that the day 4 and 5 populations that comprise more than 95% CXCR4$^+$CD117$^+$ cells have both HDE1$^+$ and HDE1$^-$ fractions suggests that they may still contain non-endodermal cell types.

HDE1$^+$ populations are enriched for endoderm potential

To determine whether HDE1 can be used to enrich definitive endoderm from mixed lineage populations, we isolated and analyzed the HDE1$^+$CXCR4$^+$ and HDE1$^-$CXCR4$^+$ fractions from a differentiated population that was induced with suboptimal concentrations of activin A (1-5 ng/ml) to ensure the presence of contaminating non-endodermal cells (50-60% CXCR4$^+$CD117$^+$; Fig. 3A). RT-qPCR analyses revealed that the HDE1$^+$CXCR4$^+$ (+ +) cells expressed significantly lower levels of the pluripotent factor *OCT4*, the mesodermal genes *MESP1*, *MEOX1*, *CD56*, the primitive streak/anterior mesoderm gene *MIXL1* and the extraembryonic endoderm marker *SOX7* than the HDE1$^-$CXCR4$^-$ (− −) cells. The reverse pattern was observed for the definitive endoderm genes *SOX17* and *FOXA2*. Likewise, the expression levels of *OCT4* and the mesoderm genes was lower in the HDE1$^+$ cells than in the presort population (Fig. 3A). The HDE1$^+$CXCR4$^+$ and HDE1$^-$CXCR4$^+$ cells showed similar expression patterns for many of these genes, a finding consistent with the fact that CXCR4 is also a marker of definitive endoderm. There were, however, several differences, including higher levels of *OCT4*, *MIXL1* and *CD56* in the HDE1$^-$CXCR4$^+$ cells than in the HDE1$^+$CXCR4$^+$ cells. Together, these findings indicate that HDE1 can be used to isolate definitive endoderm from hESC-derived populations containing mesodermal and other non-endoderm contaminants.

To investigate further the utility of HDE1 for enriching definitive endoderm able to generate hepatocytes, we next isolated and analyzed the developmental potential of HDE1^{hi}CXCR4$^+$ and HDE1$^-$CXCR4$^+$ fractions from a day 5 endoderm population that was induced in optimal conditions and consisted of more than 90% CXCR4$^+$ cells. Although highly enriched in definitive endoderm, we have previously shown that populations with these marker profiles can contain residual mesoderm that generates CD90 derivatives in hepatic differentiation cultures (Ogawa et al., 2013). Additionally, we have observed CDX2$^+$ contaminants in some of our hepatic cultures, indicating that this day 5 endoderm population is heterogeneous and contains posterior gut tube progenitors in addition to cells patterned to a hepatic fate. To determine

Development (2015) 142, 4253-4265 doi:10.1242/dev.121020

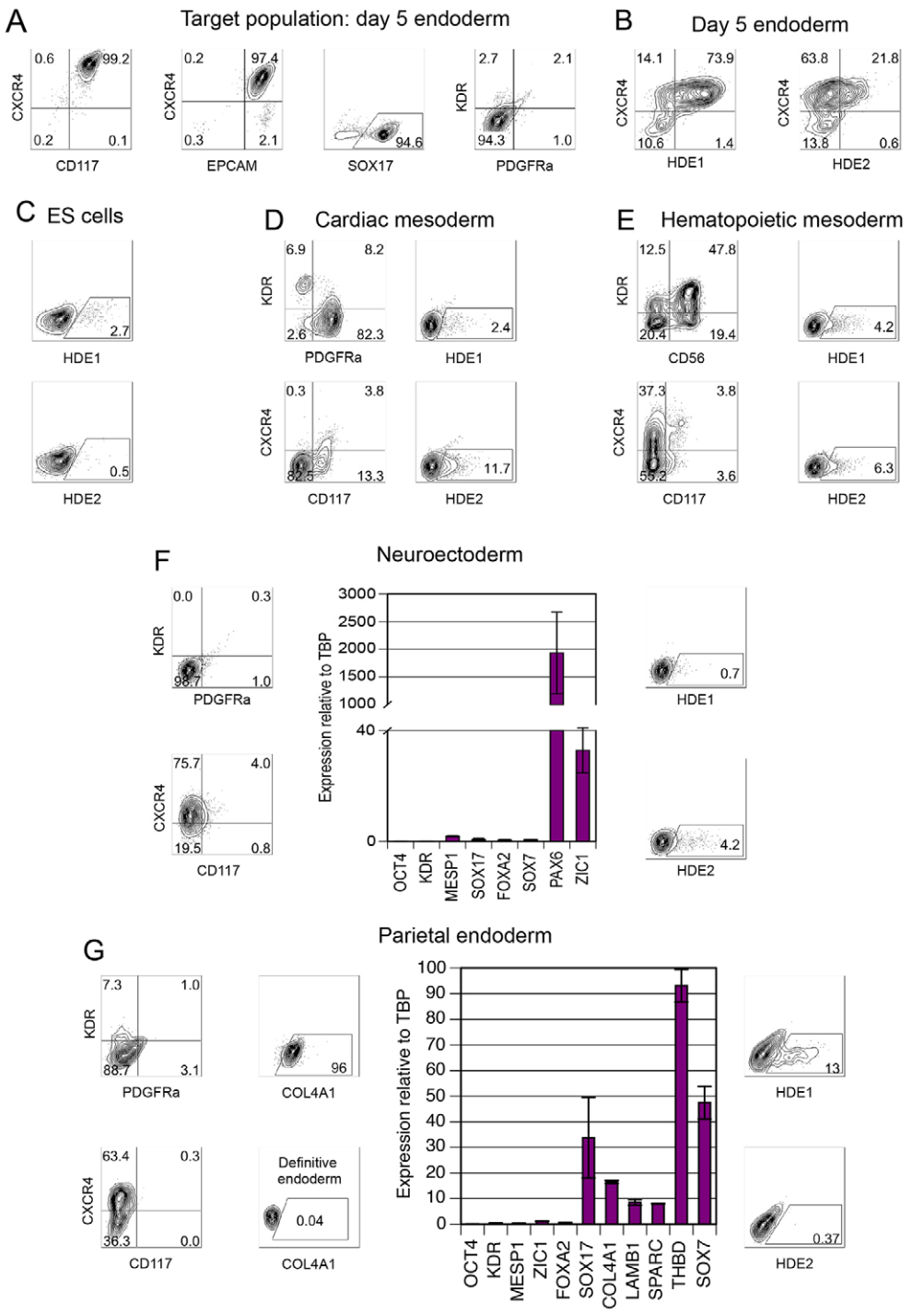

Fig. 1. Staining patterns of HDE1 and HDE2 on hESC-derived endoderm, mesoderm, ectoderm and parietal endoderm. (A) Flow cytometric analysis of the target hESC-derived endoderm population used to generate the HDE1 and HDE2 antibodies. The endoderm is characterized by the expression of CXCR4, CD117, EPCAM and SOX17 and does not express the mesodermal markers KDR and PDGFRα. (B) Flow cytometric analysis of HDE1, HDE2 and CXCR4 staining on day 5 hESC-derived endoderm. (C) Flow cytometric analysis of HDE1 and HDE2 staining on undifferentiated HES2 hESCs. (D) Flow cytometric analysis of HDE1 and HDE2 staining on hESC-derived PDGFRα^{+} cardiac mesoderm. (E) Flow cytometric analysis of HDE1 and HDE2 staining on hESC-derived KDR^{+}CD56^{+} hematopoietic mesoderm. (F) Flow cytometric analysis of HDE1 and HDE2 staining on hESC-derived KDR^{-}PDGFRα^{-}CD117^{-} neuroectoderm. RT-qPCR analyses for expression of mesoderm (*KDR* and *MESP1*), endoderm (*SOX17* and *FOXA2*), extraembryonic endoderm (*SOX7*) and neuroectoderm (*PAX6* and *ZIC1*) genes in the neuroectoderm population. Values shown for the RT-qPCR were determined relative to TBP and compared with hESCs (hESCs set at 1; *n*=3, data are represented as mean±s.e.m.). (G) Flow cytometric analyses of KDR, PDGFRα, CXCR4, CD117, COL4A1, HDE1 and HDE2 staining on hESC-derived parietal endoderm and RT-qPCR analyses of expression of the indicated genes in the population. Values shown for the RT-qPCR were determined relative to TBP and compared with hESCs levels (hESCs set at 1; *n*=3, data are represented as mean±s.e.m.). The parietal endoderm population is characterized by its specific expression of COL4A1 and high expression of *SOX17*, *COL4A1*, *LAMB1*, *SPARC*, *THBD* and *SOX7*. All FACS plots are representative results from at least three independent experiments.

whether HDE1 can be used to enrich for hepatic endoderm, the isolated fractions were cultured for 28 days in conditions to promote hepatic development and the resulting populations analyzed for the presence of albumin (ALB)$^{+}$ cells by immunostaining and intracellular flow cytometric analyses and for *ALB*, *AFP*, *CDX2* and *CD90* message by RT-qPCR. These analyses showed that the HDE1^{hi}CXCR4^{+}-derived population was enriched for ALB^{+} cells (Fig. 3B,C; P<0.01; Fig. S1) compared with the population generated from the presort cells and the HDE1^{-}CXCR4^{+} fraction. By contrast, the HDE1^{hi}CXCR4^{+}-derived population expressed lower levels of *CDX2* and *CD90* than the population that developed from the presort cells. Flow cytometric analyses confirmed the lack of CD90^{+} cells in the HDE1-derived population (Fig. S1). The *CDX2*-expressing cells segregated to the population generated from the HDE1^{-}CXCR4^{+} fraction, indicating that it is possible to separate endoderm with different fates based on HDE1 staining.

Monitoring pancreatic development with HDE1 and HDE2

To determine whether HDE1 and HDE2 stain endoderm derivatives, we next analyzed hESC-derived pancreatic and hepatic populations differentiated using previously described protocols (Nostro et al., 2011; Ogawa et al., 2013). To generate pancreatic lineage cells, the day 7 population was treated with FGF10 for 3 days to pattern a foregut fate and then with the

Development (2015) 142, 4253-4265 doi:10.1242/dev.121020

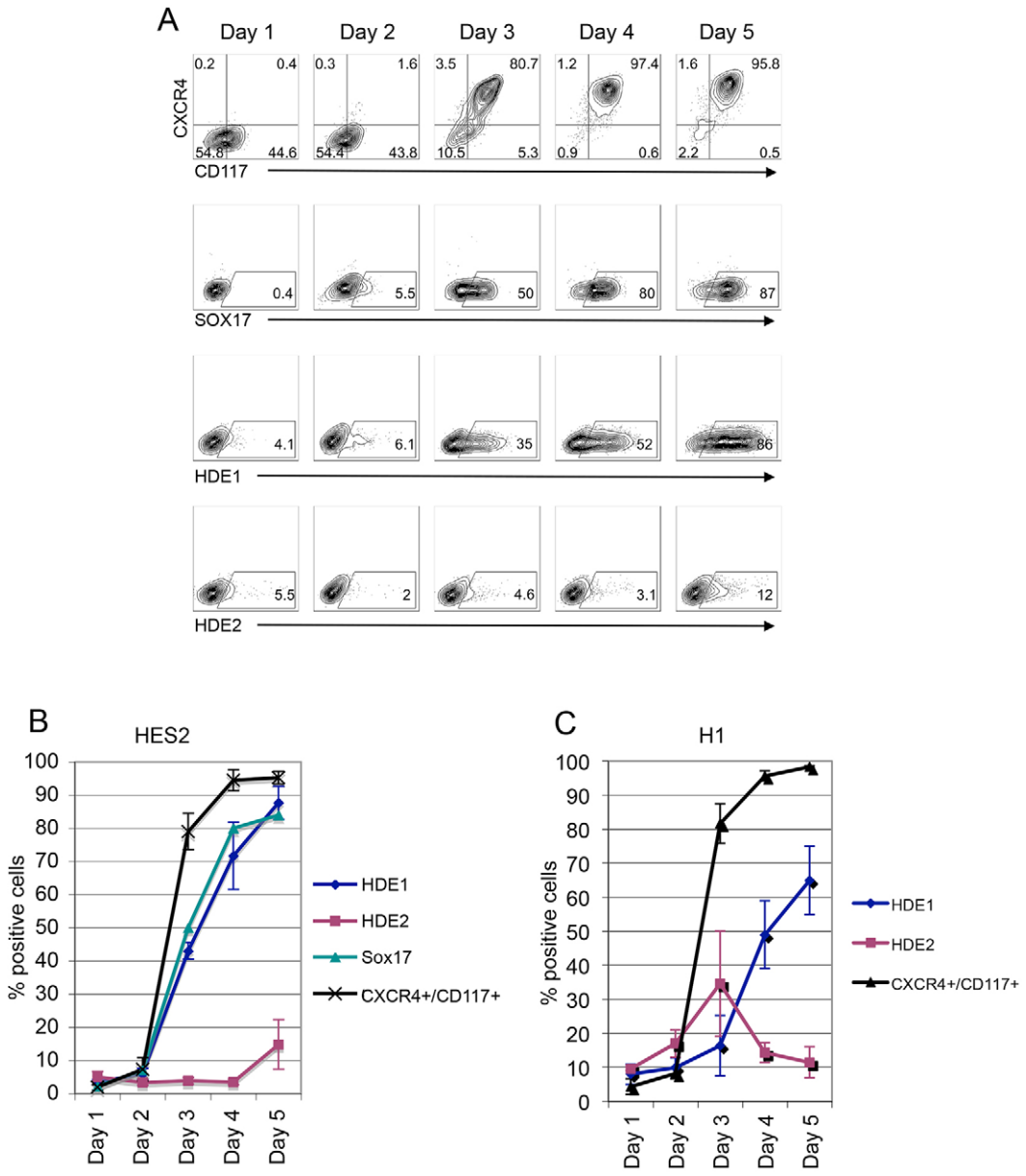

Fig. 2. Kinetics of HDE1 and HDE2 staining during definitive endoderm induction from hESCs. (A) Representative flow cytometry analyses of the staining patterns of CXCR4/CD117, SOX17, HDE1 and HDE2 on HES2 hESC-derived endoderm populations between days 1 and 5 of differentiation. (B) Kinetics of HDE1, HDE2, SOX17 and CXCR4/CD117 staining during endoderm induction of HES2 hESCs (n=3, data are represented as mean±s.e.m.). (C) Kinetics of HDE1, HDE2 and CXCR4/CD117 staining during endoderm induction of H1 hESCs (n=3, data are represented as mean±s.e.m.).

combination of retinoic acid (RA), cyclopamine and noggin for another 3 days to induce the development of PDX1$^+$ progenitors. These progenitors were matured to c-peptide$^+$ cells by culture in the presence of the TGFβ and BMP inhibitors SB-431542 and noggin for an additional 4 days. At this stage, the cells were maintained in basal medium for 8 days. This protocol preferentially promotes the generation of first transition, polyhormonal cells. As shown in Fig. 4A and Fig. S2A, the endoderm population remained HDE1$^+$ through the FGF10 patterning stage to day 10. After pancreatic induction (day 13), however, HDE1 staining decreased dramatically, indicating that the specified progenitors are initially HDE1$^-$. An HDE1$^+$ population emerged by day 15 and persisted throughout the 20-day time course of the experiment. An HDE2$^+$ population was detected at day 7. Beyond this stage, the proportion of positive cells declined and remained low throughout the 20 day differentiation period (Fig. 4A; Fig. S2A). Flow cytometric and immunostaining analyses of the differentiated populations at day 25 of culture revealed that HDE1 did not stain the c-peptide$^+$ polyhormonal cells, but rather marked clusters of large cells present at this stage (Fig. 4B). These cells may represent the emerging exocrine lineage, because analyses of fetal and adult pancreas revealed that HDE1 stains the exocrine compartment of these tissues (Fig. 4C,D). HDE1 also stains ductal cells within the fetal and adult pancreas (data not shown) and a human pancreatic duct epithelial cell line HPDE6 (Ouyang et al., 2000; Fig. 4E; Fig. S2B). Consistent with our observations in hESC-derived pancreas cultures, the majority of exocrine and endocrine cells in the fetal and adult pancreas were HDE2$^-$. HDE2 did stain some ductal cells in the adult pancreas (Fig. 4C,D). HDE2 also stained a subset of HPDE6 cells (Fig. 4E; Fig. S2B). These findings show that

Development (2015) 142, 4253-4265 doi:10.1242/dev.121020

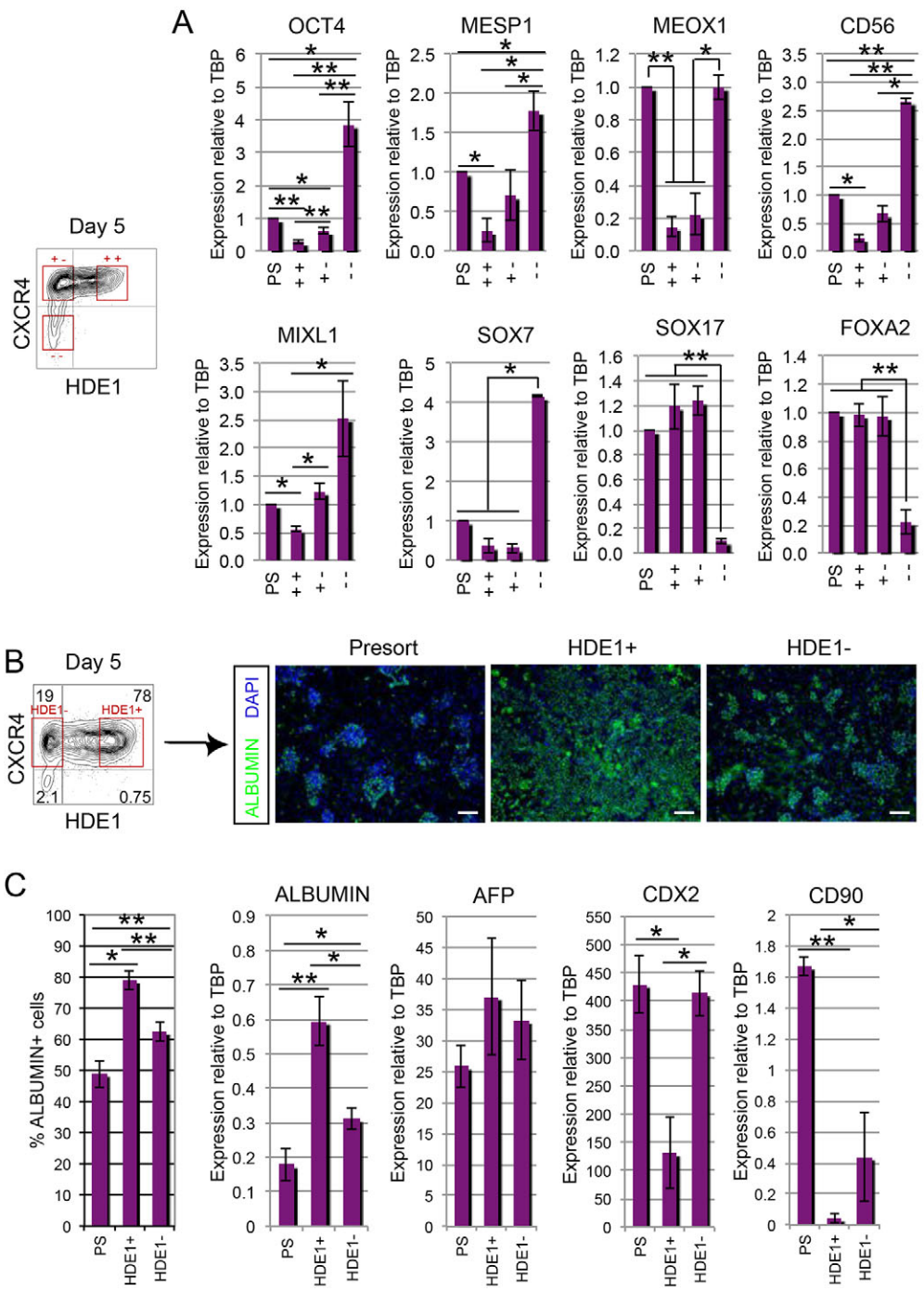

Fig. 3. Isolation and characterization of HDE1$^+$ populations.
(A) Representative flow cytometric profile of CXCR4 and HDE1 staining in an HES2-derived day 5 EB population induced with suboptimal levels of activin A (5 ng/ml). Red boxes indicate the three subpopulations isolated by FACS for RT-qPCR analyses for expression of the pluripotency marker *OCT4*, the mesoderm markers *MESP1*, *MEOX1* and *CD56*, the mesendoderm marker *MIXL1*, the extra-embryonic endoderm marker *SOX7* and the endoderm markers *SOX17* and *FOXA2*. Values shown were determined relative to TBP and compared with presort levels, which were set at 1 (n=3, data are represented as mean±s.e.m. *P<0.05; **P<0.01). (B) Left: representative flow cytometric profile of CXCR4 and HDE1 staining in an HES2-derived day 5 EB population induced in optimal endoderm induction conditions. Red boxes indicate the two subpopulations isolated for functional analyses. The presort and CXCR4$^+$HDE1$^-$ and CXCR4$^+$HDE1$^+$ cells were cultured in hepatocyte conditions for 28 days. The resulting populations were analyzed by immunocytochemistry (right) for expression of ALB (green). Nuclei were visualized by DAPI staining. Scale bar: 200 µm. (C) Intracellular flow cytometric analysis of ALB$^+$ cells (left panel) in populations generated from the presort and CXCR4$^+$HDE1$^-$ and CXCR4$^+$HDE1$^+$ fractions (described in B) after 33 days of culture in hepatic conditions. RT-qPCR analysis of *ALB*, *AFP*, *CDX2* and *CD90* expression in the day 33 hepatic populations (n=4, data are represented as mean±s.e.m. *P<0.05; **P<0.01). Values shown were determined relative to TBP and compared with fetal liver (FL set at 1).

HDE1 staining declines as endoderm is induced to a pancreatic fate. After emergence of the pancreatic lineages, the HDE1$^+$ population is restricted to the non-endocrine fraction of the population that may represent the developing exocrine and ductal lineages.

Monitoring hepatic development with HDE1 and HDE2

To monitor hepatic development, we used a modification of our previous protocol, in which the cells are induced as a monolayer rather than EBs (Ogawa et al., 2015). Given that activin A is already present at day 0 in this format, the kinetics of endoderm induction, as demonstrated by the staining patterns of CXCR4, CD117, EPCAM and HDE1, are accelerated by approximately 24 h compared with those observed in the EBs (Fig. S3). At day 7 of monolayer culture, the population was specified to a hepatic fate by culture in the presence of BMP4 and basic fibroblast growth factor (bFGF; FGF2) for 6 days. The specified population was then cultured in hepatocyte growth factor (HGF), oncostatin M and dexamethasone to promote maturation and the development of ALB$^+$ cells. With this protocol, ALB$^+$ cells are detected by day 16 of differentiation. By day 24, the majority of the population is ALB$^+$, although the proportion of positive cells varies between cell lines (Fig. 5A; Fig. S4A,D). We have recently demonstrated that this ALB$^+$ population represents the hepatoblast stage of liver development (Ogawa et al., 2015). With the HES2 cell line, the entire BMP4/bFGF-specified population remained HDE1$^+$ between days 7 and 14 of differentiation. The proportion of HDE1$^+$ cells

Development (2015) 142, 4253-4265 doi:10.1242/dev.121020

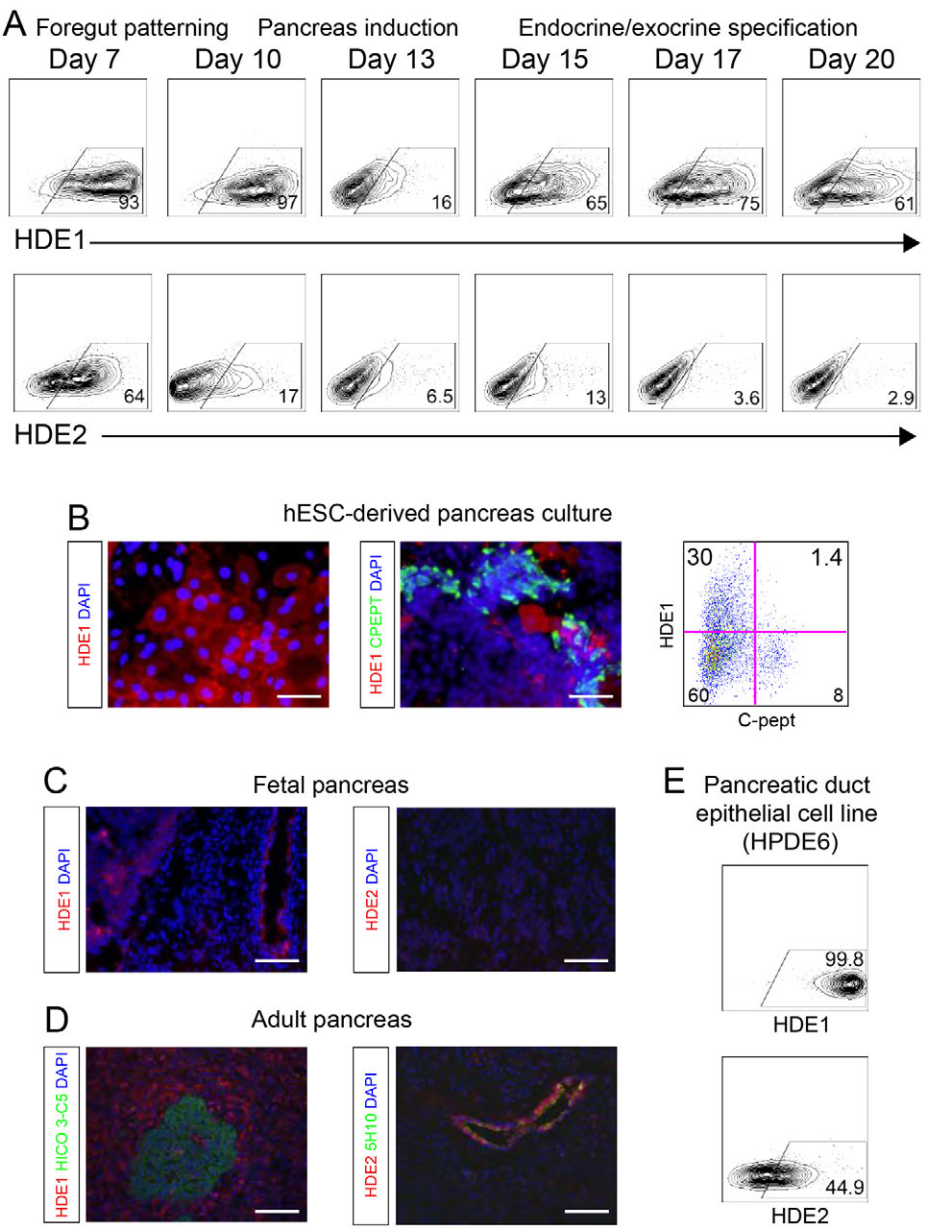

Fig. 4. HDE1 and HDE2 staining patterns on hESC-derived pancreatic cells and pancreatic tissue. (A) Representative flow cytometric analyses of HDE1 and HDE2 staining patterns of HES2 hESC-derived populations undergoing pancreatic differentiation between days 7 and 20 of culture. Similar patterns were found in three independent experiments (Fig. S1A). (B) Immunocytochemistry analyses of HDE1$^+$ (red) and c-peptide$^+$ (green) cells in HES2-derived pancreatic populations at day 25 of differentiation. Scale bars: 100 µm. Representative flow cytometric analysis of the frequency of HDE1$^+$ and c-peptide$^+$ cells in comparable day 25 pancreatic populations (right panel). (C) Immunocytochemistry analyses of HDE1$^+$ (red, left panel) and HDE2$^+$ (red, right panel) cells in human fetal pancreas (week 40 gestation). Nuclei are visualized by DAPI staining. Scale bars: 100 µm. (D) Immunocytochemistry analyses of HDE1$^+$ (red, left panel) and HDE2$^+$ (red, right panel) cells in normal adult pancreas. Ductal structures are indicated by staining with the ductal antibody 5H10 (green, right panel) and islets with the islet antibody HICO 3C5 (green, left panel). Nuclei are visualized by DAPI staining. Scale bars: 100 µm. (E) Representative flow cytometric analyses of HDE1 and HDE2 staining on the pancreatic duct epithelial cell line HPDE6. Similar patterns were found in three independent experiments (Fig. S1B).

began to decline with the emergence of ALB$^+$ cells (day 16) and continued to decline to represent approximately half of the population at day 24 (Fig. 5A; Fig. S4B). The proportion of HDE2$^+$ cells in the culture increased between days 7 and 10, declined until day 12-14 and then increased with the development of the ALB$^+$ cells (Fig. 5A; Fig. S4C). By day 24 of culture, the majority of the population was HDE2$^+$. Similar trends were observed in the H9 hESC-derived populations, although the changes in staining patterns were much more dramatic (Fig. 5B; Fig. S4B,C). As observed with the HES2-derived cells, the early H9 BMP4/bFGF-specified population (day 10) was HDE1$^+$. Beyond this stage, however, the proportion of HDE1$^+$ cells dropped dramatically and remained low (<5%) for the duration of the culture (Fig. 5B; Fig. S4B). The proportion of HDE2$^+$ cells declined until day 12, then increased to represent more than 95% or the population by day 24. At this stage, 90% of the cells in the H9-derived population were ALB$^+$ (Fig. S4C,D). Together, these findings indicate that HDE2, but not HDE1, tracks with the emerging hESC-derived hepatic lineage.

In order to characterize further the hepatic staining patterns of these antibodies, we analyzed fetal and adult liver and two liver carcinoma cell lines, Huh7 and HepG2. Fetal and adult hepatocytes were HDE2$^+$, as determined by immunostaining. Neither population stained with HDE1 (Fig. 6A,B). Flow cytometric analyses were consistent with these findings and showed that HDE2 but not HDE1 stained primary hepatocytes, the entire Huh7 population and a portion of the HepG2 cell line (Fig. 6C,D).

Given these staining patterns, our interpretation of the persistence of HDE1$^+$ cells in the HES2-derived hepatic population is that they are likely to represent non-hepatic contaminants. Findings from cell sorting studies supported this interpretation and showed that the HDE1$^+$ fraction isolated from day 26 cultures expressed lower levels of *ALB* mRNA and contained significantly fewer ALB$^+$ cells than the HDE1$^-$ fraction (Fig. 6E; P<0.01). Immunostaining analyses of

Development (2015) 142, 4253-4265 doi:10.1242/dev.121020

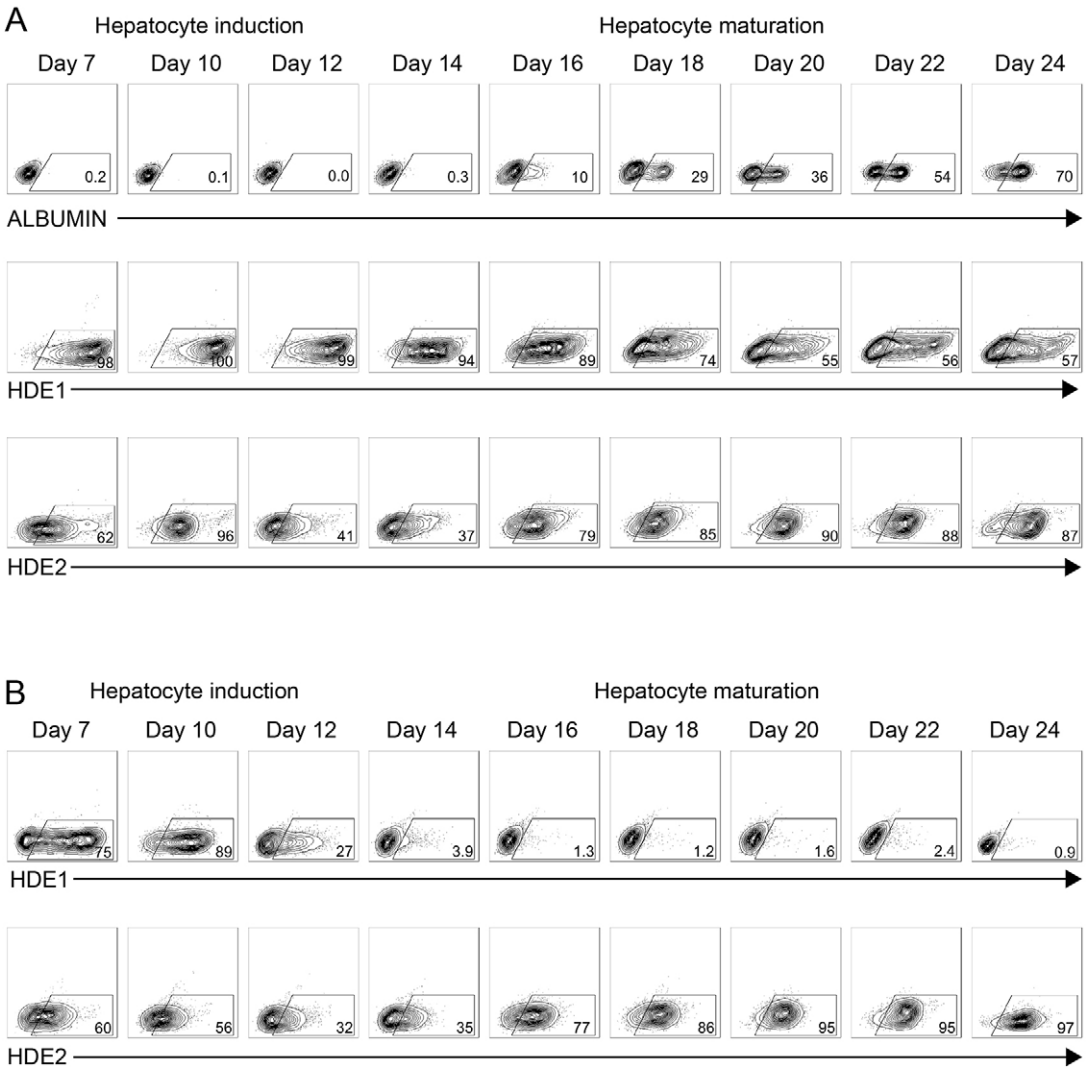

Fig. 5. Kinetics of HDE1 and HDE2 staining during hepatic differentiation of hESCs. (A) Representative flow cytometric analyses of ALB and HDE1 and HDE2 staining patterns of HES2 hESC-derived populations at different stages of hepatic differentiation. (B) Representative flow cytometric analyses of HDE1 and HDE2 staining patterns of H9 hESC-derived populations at different stages of hepatic differentiation. Similar patterns were found in three independent experiments (Fig. S3).

the day 26 hESC-derived population revealed that HDE1 stained large ALB$^-$ and AFP$^-$ cells, consistent with the interpretation that they are not hepatic lineage cells (Fig. 6F). As the levels of FOXA2 were similar in the two populations, the cells are likely to represent a non-hepatic endoderm-derived lineage (Fig. 6E).

HDE1 definitive endoderm staining patterns are correlated with hepatic potential

Previous studies have shown that prolonged activin signaling during endoderm induction from hPSCs enhances the hepatic potential of the population (Ogawa et al., 2013). Given that HDE1 staining increases over time during activin induction (Fig. 2; Fig. S3), we next wanted to determine whether the staining patterns of HDE1 are correlated with these differences in potential. To address this, we analyzed H9 hESC-derived endoderm that was induced with activin for 3, 5, 7 or 9 days for the proportion of HDE1$^+$, CXCR4$^+$ and CD117$^+$ cells. These different endoderm populations were specified to a hepatic fate with bFGF and BMP4 following the activin induction step and matured to the ALB$^+$ hepatoblast stage as described above. The different populations were analyzed for the presence of ALB$^+$ and HDE2$^+$ cells 19 days following the end of the endoderm induction step (DE), at the beginning of hepatic specification. As shown in Fig. 7A, 85% of the cells were CXCR4$^+$ and CD117$^+$ within day 3 of differentiation and by day 5 more than 95% were positive. As observed with the HES2 and H1 cell lines (Fig. 2; Fig. S3), the emergence of the H9 HDE1$^+$ population was slower than the CXCR4$^+$CD117$^+$ population, as only 37% of the cells at day 3 stained with the antibody. The proportion of HDE1$^+$ cells increased over the next 6 days of induction to represent 96% of the population by day 9 (Fig. 7A; Fig. S5). The size of the ALB$^+$ population detected 19 days after specification showed a good correlation with the degree of HDE1 staining at the endoderm stage of differentiation (Fig. 7A; Fig. S5). Notably, the levels of HDE2 staining in the final stage also correlated well with the size of the ALB$^+$ population, consistent with our earlier findings that it tracks with the developing hepatocyte-like cells (Fig. 7A).

Kinetic analyses showed that the proportion of HDE1$^+$ cells in all induced populations declined to less than 5% following specification with bFGF and BMP4 (Fig. 7B). The overall patterns of HDE2 staining were similar between the different

Development (2015) 142, 4253-4265 doi:10.1242/dev.121020

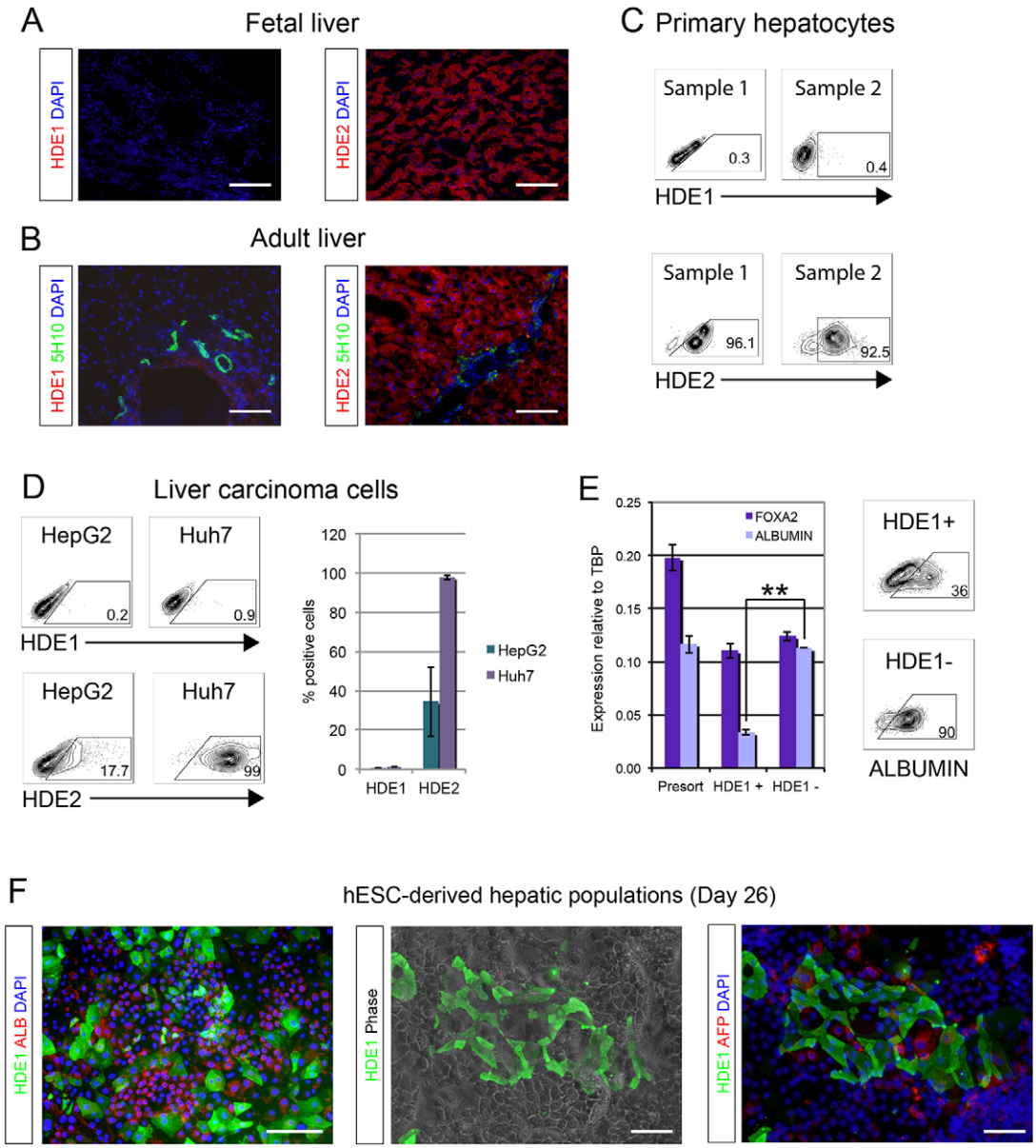

Fig. 6. HDE1 and HDE2 staining patterns on human liver tissue, cell lines and hESC-derived hepatic populations. (A) Immunocytochemistry analyses of HDE1$^+$ (red, left panel) and HDE2$^+$ (red, right panel) cells in human fetal liver (week 20 gestation). Nuclei are visualized by DAPI staining. Scale bars: 100 µm. (B) Immunocytochemistry analyses of HDE1$^+$ (red, left panel) and HDE2$^+$ (red, right panel) cells in normal adult liver. Ductal structures are stained with the ductal antibody 5H10 (green) and nuclei visualized by DAPI. Scale bars: 100 µm. (C) Flow cytometric analysis of HDE1 and HDE2 staining on two independent samples of human primary hepatocytes. (D) Representative flow cytometric analyses of HDE1 and HDE2 staining on human fetal (HepG2) and adult (Huh7) liver carcinoma cells (left). Graph (right) shows the combined values of three independent experiments (n=3, data are represented as mean±s.e.m.). (E) RT-qPCR analysis of *FOXA2* and *ALB* expression in presort and in HDE1$^+$ and HDE1$^-$ cells isolated from day 26 HES2-derived hepatic populations (left). Values were determined relative to TBP and compared with fetal liver (FL set at 1; n=3, data are represented as mean±s.e.m. $^{**}P$<0.01). Flow cytometry analysis of ALB expression in HDE1$^+$ and HDE1$^-$ cells isolated from day 26 HES2-derived hepatic populations (right). (F) Immunocytochemistry analyses of HDE1$^+$ (green), ALB$^+$ (red, left picture) and AFP$^+$ (red, right picture) cells in day 26 HES2-derived hepatic populations (right pictures, scale bars: 200 µm; left picture, scale bar: 100 µm).

groups. At the early stages of differentiation (days 3-5), the proportion of HDE2$^+$ cells was consistently higher in the H9-derived populations than in those generated from either HES2 or H1 hESCs. The proportion of HDE2$^+$ cells declined within 5-7 days of bFGF/BMP specification and then increased to reach maximal levels between days 13 and 19 (Fig. 7C). The HDE2 profiles in the different groups at the DE+19 days time point reflected the hepatic potential of the population, as determined by the proportion of ALB$^+$ cells (Fig. 7A). RT-qPCR analysis of the different populations 19 days after endoderm specification showed that those derived from the 5-, 7- and 9-day-induced endoderm expressed higher levels of *ALB* than the cells derived from the 3-day-induced endoderm (Fig. 7D; P<0.05). The expression patterns of *CD90* and *CDX2* were opposite to that of *ALB*, indicating that populations derived from endoderm induced for shorter periods of time contained contaminating CD90$^+$ mesenchymal cells and CDX2$^+$ posterior gut tube cells (Fig. 7D; P<0.05).

Analyses of two hiPSC lines, BJ and MSC-iPS1, revealed similar correlations between HDE1 endoderm staining patterns and hepatic potential. With both cell lines, populations with the highest proportion

Development (2015) 142, 4253-4265 doi:10.1242/dev.121020

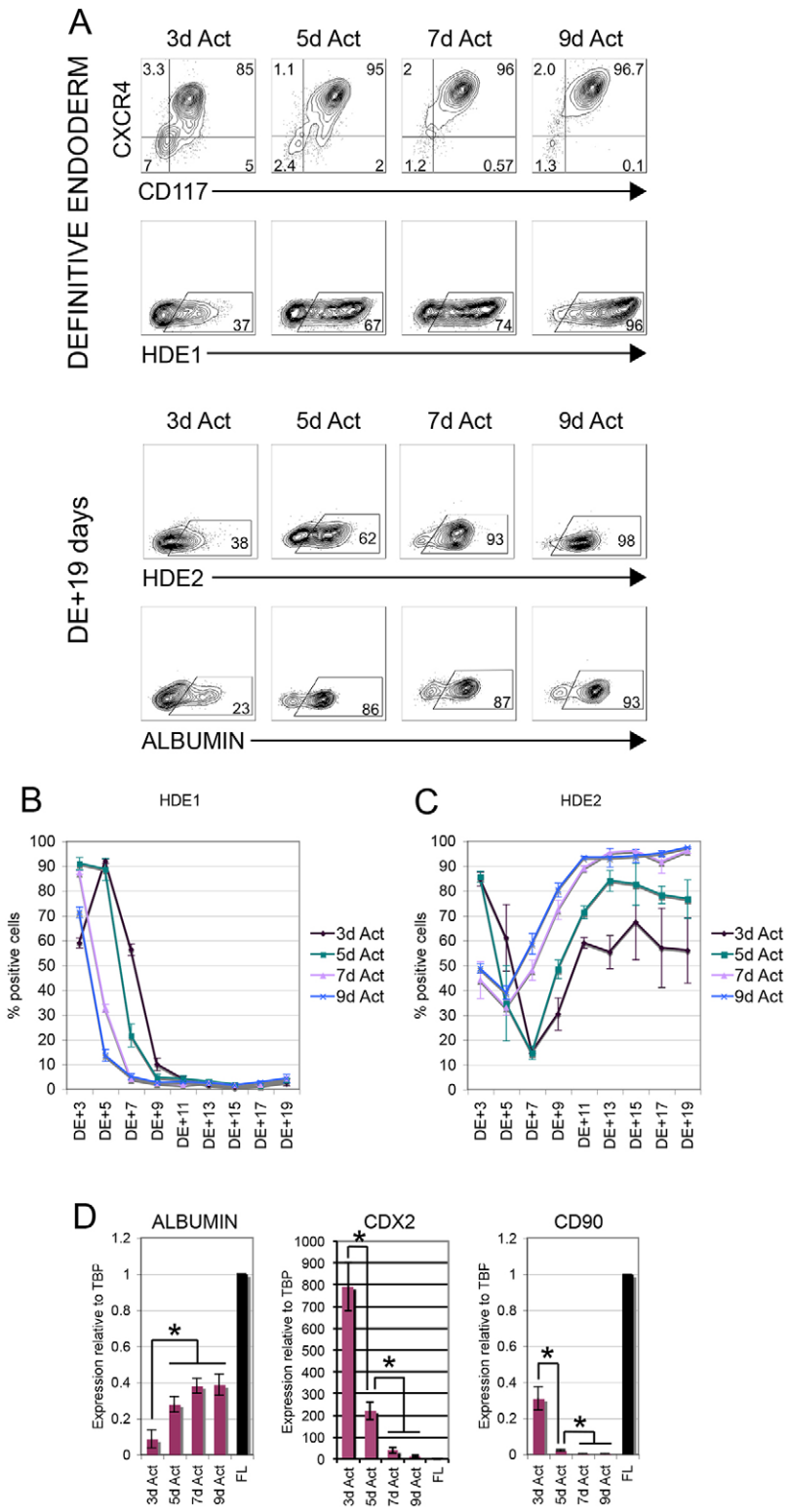

Fig. 7. Hepatic potential of hESC-derived endoderm is correlated with HDE1 staining patterns. (A) Upper two rows: representative flow cytometric analysis showing the proportion of CXCR4$^+$, CD117$^+$ and HDE1$^+$ cells in H9 hESC-derived endoderm populations induced with activin A for the indicated period of time (in days, d). Similar patterns were found in three independent experiments (Fig. S4). Lower two rows: representative flow cytometric analysis showing the proportion of HDE2$^+$ and ALB$^+$ cells in hepatic cultures generated from endoderm induced for the indicated periods of time. Cells were analyzed 19 days after the endoderm stage (DE+19 days). (B) Flow cytometric analyses of HDE1 staining at different stages of hepatocyte development in populations generated from the endoderm populations induced for different periods of time (n=3, data are represented as mean±s.e.m.). (C) Flow cytometric analyses of HDE2 staining at different stages of hepatocyte development in populations generated from the endoderm populations induced for different periods of time. (D) RT-qPCR analyses of *ALB*, *CDX2* and *CD90* expression in the hepatic populations (DE+19 days) generated from the endoderm induced with activin A for different periods of time. FL, fetal liver. Values were determined relative to TBP and compared with fetal liver (FL set at 1; n=3, data are represented as mean±s.e.m. *P<0.05).

of ALB$^+$ cells were generated from endoderm that was more than 90% HDE1 positive (Fig. S6A; Fig. S7A). Seven days of activin induction was sufficient to induce optimal hepatic endoderm populations from both hiPSC lines (Fig. S6; Fig. S7). Molecular analyses showed that hepatic populations generated from day 3- and 5-induced BJ hiPSC endoderm expressed significantly lower levels of *ALB* and higher levels of *CD90* and *CDX2* than populations generated from day 7- and 9-induced endoderm (Fig. S6C; P<0.05). Similar patterns were observed for the MSC-iPS1-derived populations, as cells generated from the day 7-induced endoderm expressed higher levels of *ALB* and lower levels of *CD90* and *CDX2* than those derived from the day 3-induced endoderm (Fig. S7C; P<0.01 and P<0.05, respectively). Taken together, these findings demonstrate that the staining patterns of HDE1 reflect differences in the hepatic potential of hPSC-derived endoderm and, as such, can be used to optimize the induction of hepatic endoderm from different hPSC lines.

Development (2015) 142, 4253-4265 doi:10.1242/dev.121020

DISCUSSION

The efficient and reproducible production of highly enriched hPSC-derived populations is dependent on our ability to recapitulate key stages of embryonic lineage development in the differentiation cultures. The earliest step in this process, germ layer induction, is among the most important, because inefficiencies at this stage result in mixed populations, with contaminants from other germ layers. Advances over the past decade have provided insights into the signaling pathways that regulate both the endoderm induction and subsequent steps, allowing for the generation of a range of derivative cell types, including pancreatic insulin-producing cells, hepatocytes, intestinal cells and lung cells (D'Amour et al., 2005; Gouon-Evans et al., 2006; Huang et al., 2014; Ogawa et al., 2013; Pagliuca et al., 2014; Rezania et al., 2014; Si-Tayeb et al., 2010; Spence et al., 2011). Optimization of these differentiation steps is essential for the efficient production of these cells and is ideally monitored quantitatively by flow cytometric analyses of the expression of cell type and/or lineage specific surface makers. Currently, the efficiency of endoderm induction is routinely assessed by coexpression of CXCR4, CD117 and/or EPCAM. Although useful, these markers are neither endoderm specific nor are they able to distinguish subpopulations with different fates. The two antibodies generated and characterized in the present study, HDE1 and HDE2, provide new tools for monitoring endoderm induction and hepatic specification.

At the early stages of development, HDE1 shows remarkable endoderm specificity and is able to discriminate endoderm and non-endoderm cell types in the differentiating populations. In the suboptimally induced population, HDE1 staining marked the definitive endoderm fraction and enabled the isolation of these cells from the contaminating mesoderm, undifferentiated hESCs and other non-endoderm cell types. Importantly, HDE1 staining also revealed the presence of $CD90^+$ mesoderm contaminants in optimally induced endoderm populations that were not detected based on CXCR4 staining. These findings confirm our previous studies that showed that $CXCR4^+CD117^+$ endoderm displays the potential to generate $CD90^+$ cells and suggest that most populations induced with the combination of Wnt and activin A may contain low levels of this mesoderm. Our analyses of the day 5 endoderm population indicate that HDE1 staining can also distinguish subtypes of endoderm, because the population derived from the $CXCR4^+HDE1^+$ fraction was enriched for hepatic potential and depleted of *CDX2*-expressing cells, whereas the $CXCR4^+HDE1^-$-derived population contained *CDX2*-expressing cells and a lower proportion of ALB^+ cells. Taken together, these observations indicate that HDE1 can be used to segregate hepatic endoderm from mesoderm and non-hepatic endoderm in optimally induced $CXCR4^+$ populations.

Previous studies have shown that sustained activin and/or nodal signaling is essential for optimal generation of endoderm with hepatic potential (Ogawa et al., 2013; Si-Tayeb et al., 2010; Toivonen et al., 2013a). The duration of this induction step in our culture conditions was found to vary between hPSC lines, and optimal timing could be determined only by measuring the proportion of ALB^+ cells at day 24 of culture. Our observation that the extent of HDE1 staining is correlated with hepatic potential provides a new and rapid method to optimize this induction step. We observed that endoderm populations generated by sustained activin signaling (days 7-9) and composed of >90% $HDE1^+$ cells display high hepatic potential and a reduced capacity to generate *CD90*- and *CDX2*-expressing cells compared with populations containing a lower proportion of $HDE1^+$ cells induced for a shorter period of time (days 3-5). These findings are in line with those of Spence et al. (2011), who showed that prolonged induction of hPSC-derived endoderm with activin led to a reduction in intestinal potential. Whether or not other patterns of HDE1 staining are correlated with other endoderm fates is currently under investigation. With our ability to isolate highly enriched $HDE1^+$ endoderm populations at different stages, it will be possible to investigate the molecular and epigenetic changes associated with hepatic endoderm development.

The staining patterns of HDE1 and HDE2 in the later stage specified populations show remarkable diversity and highlight potential new uses of these antibodies. For instance, the staining patterns of HDE1 in the pancreatic tissue and populations strongly suggest that this antibody marks the emerging exocrine and ductal progenitors in the hPSC differentiation cultures. If further analyses confirm this, it will be possible to monitor the efficiency of endocrine versus exocrine induction in the differentiation cultures and to deplete the population of non-endocrine cells. Additionally, it will be possible to isolate the early stage exocrine and ductal progenitors and evaluate their developmental potential, both *in vitro* and following transplantation *in vivo*. Although the staining pattern of HDE2 was somewhat variable in the early endoderm stages, it did track well with the emerging ALB^+ population, suggesting that this antibody uniquely recognizes the developing hepatocyte lineage. Our analyses of liver tissue demonstrated that this specificity for the hepatocyte lineage was retained through fetal and adult life. Given these patterns, HDE2 can be used to monitor the efficiency of hepatic development in hPSC differentiation cultures and to isolate hepatic cells from mixed populations.

A number of recent studies have identified other cell surface markers and developed other complementary techniques to monitor the efficiency of endoderm induction. With respect to markers, two integrins, CD49e and CD51, have recently been shown to be expressed on hPSC-derived definitive endoderm (Brafman et al., 2013). However, as with CXCR4, CD117 and EPCAM, neither is endoderm specific because both are expressed on the $CXCR4^-$ population. In preliminary analyses, we found that CD49e was expressed on entire suboptimally induced populations (70% $CXCR4^+CD117^+$) between days 3 and 7 of differentiation, confirming that expression of this integrin is not endoderm specific. Using a different approach, Iwashita et al. (2013) showed that the levels of secreted cereberus 1 (CER1) quantified by enzyme-linked immunosorbent assay were correlated with the amount of endoderm in the culture. Although informative, the analyses cannot distinguish between CER1 secreted from visceral and definitive endoderm, and the approach cannot be used to enrich populations of interest. Pan et al. (2011) developed a technique (referred to as transcription factor fluorescence-activated cell sorting, tfFACS) to sort subpopulations of fixed endodermal cells based on transcription factor expression. This method has the advantage of being able to isolate and analyze specific subsets of endoderm based on differential expression of transcription factors. However, as cells are fixed in the process, this approach cannot be used to carry out functional analyses of the isolated populations.

In summary, we have generated and characterized two antibodies, HDE1 and HDE2, which display interesting and informative staining patterns on hPSC-derived endoderm and derivative populations. With these reagents, we were able to develop new stringent flow cytometry-based analyses for monitoring the efficiency of endoderm induction and, in doing so, demonstrate that populations considered to be highly enriched for endoderm by current criteria can contain residual mesoderm potential. Additionally, we showed that with the combination of staining

Development (2015) 142, 4253-4265 doi:10.1242/dev.121020

patterns of the two antibodies, it is now possible to monitor the optimization of two stages of hepatic development, endoderm induction and hepatic specification, by flow cytometry. Together, these findings highlight the importance of stage and lineage specific markers for developing efficient and reproducible differentiation strategies for the generation of functional hPSC-derived cell types.

MATERIALS AND METHODS

Generation of hESC-derived endoderm for production of monoclonal antibodies

HES2 hESCs were differentiated as embryoid bodies (EBs) in low-cluster six-well plates (4×10^5 cells/ml) in serum-free differentiation (SFD) medium (Gouon-Evans et al., 2006) supplemented with 2 mM L-glutamine (Gibco-BRL), 1 mM ascorbic acid (Sigma), 4×10^{-4} M monothioglycerol (MTG; Sigma) and 10 ng/ml BMP4 (R&D Systems). After 24 h (day 1), the medium was changed to SFD supplemented with 2 mM glutamine, 0.5 mM ascorbic acid, 4×10^{-4} M MTG, 0.25 ng/ml BMP4, 2.5 ng/ml bFGF, 100 ng/ml activin A for 3 days. On day 4, EBs were transferred to fresh day 1 medium with 10 ng/ml vascular endothelial growth factor. The resulting day 5 population was harvested and used for immunization for the generation of antibodies.

Antibody production

Monoclonal antibodies were generated using standard polyethylene-mediated fusion technology (Köhler and Milstein, 1975). Briefly, BALB/c mice were immunized three times with day 5 HES2 hESC-derived definitive endoderm. Immunizations were conducted at intervals of 3 weeks and, for each immunization, mice received approximately 0.5×10^6 cells delivered intraperitoneally. Imject Alum (Thermo Scientific) was used as an adjuvant/carrier. Four days after the final immunization, animals were humanely euthanized and their spleens removed for hybridoma generation. Splenocytes were fused with SP2/0 Ag14 myeloma cells using standard PEG, and successfully fused cells were cloned using ClonaCell-HY media (Stem Cell Technologies). Approximately 600 isolated clones per fusion were transferred to liquid media in 96-well plates, and supernatants from those wells were collected for screening, with screening for cell surface reactivity performed as described below (flow cytometry and cell sorting).

Maintenance and differentiation of HESCs and hiPSCs

hESCs and iPSCs were cultured on irradiated mouse embryonic fibroblasts in hESC medium, as previously described (Kennedy et al., 2007). For pancreatic differentiation, hESCs were first passaged onto Matrigel-coated dishes for 24 h to deplete the feeder cells. hESCs and hiPSCs were then dissociated using collagenase B (1 mg/ml) for 20 min, followed by a 1-2 min trypsin-EDTA (0.05%) treatment. Single cell suspensions were seeded in low-cluster dishes (Corning) at a density of 4×10^5 cells/ml to generate EBs. Pancreatic differentiation was then carried out as described by Nostro et al. (2011). Briefly, EBs were treated with 100 ng/ml activin to generate definitive endoderm (see above). At day 5, the EBs were dissociated and the cells plated on gelatin at a concentration of 130,000 cells/cm^2, in 50 ng/ml activin A. On day 7, the posterior foregut was patterned with 100 ng/ml FGF10 for 3 days. The pancreatic progenitors were then induced by 50 ng/ml noggin, 250 nM KAAD-cyclopamine and 2 µM all-trans retinoic acid, for 3 days. Pancreatic maturation was then achieved by keeping the cells in 6 µM SB431542 and 50 ng/ml noggin. For liver differentiation, the definitive endoderm was induced either as EBs (as described above) or as a monolayer (Ogawa et al., 2015). For the monolayer induction, the hESCs were passaged on Matrigel-coated dishes and cultured for 24 h at a concentration of 40,000 cells/cm^2 in hESC medium. Following this step, the cells were induced with 100 ng/ml activin A (R&D Systems) and 1 µM CHIR 99021 for 1 day in RPMI supplemented with 2 mM glutamine (Gibco-BRL) and 4.5×10^{-4} M MTG (Sigma), then with 100 ng/ml activin A, 1 µM CHIR 99021 and 2.5 ng/ml bFGF (R&D Systems) for 1 day in RPMI supplemented with glutamine, 0.5 mM ascorbic acid (Sigma) and MTG. The medium was then changed to 100 ng/ml activin A and 2.5 ng/ml bFGF for an additional day in RPMI supplemented with glutamine, ascorbic acid and MTG. For longer activin exposure, the medium was changed on days 3, 5 and 7 and replaced with 100 ng/ml activin A and 2.5 ng/ml bFGF in SFD supplemented with glutamine, ascorbic acid and MTG.

Hepatic differentiation was carried out as previously described (Ogawa et al., 2013). Briefly, hepatic specification was induced from the definitive endoderm (DE) with 40 ng/ml bFGF (20 ng/ml for HES2) and 50 ng/ml BMP4, for 6 days (DE+6 days). At DE+6 days, the medium was changed to 20 ng/ml HGF, 40 ng/ml dexamethasone and 20 ng/ml oncostatin M, until DE+16 days. At DE+16 days, HGF was removed from the culture medium.

For differentiation of cardiac mesoderm and cardiomyocytes, hESCs were processed as described by Kattman et al. (2011). Induction of hematopoietic mesoderm was carried out as described previously (Kennedy et al., 2012). Differentiation of neuroectoderm was performed as described by Chambers et al. (2009).

Flow cytometry and cell sorting

Cells were trypsinized and resuspended in PBS+10% Knockout serum replacement (Gibco). For cell surface proteins, cells were stained in PBS+10% Knockout serum replacement. For intracellular staining, cells were first fixed in 2-4% paraformaldehyde in PBS for 20 min at room temperature. Cells were then permeabilized on ice in 90% methanol in PBS for 20 min, and stained in PBS+0.3% bovine serum albumin (BSA)+0.3% Triton X-100 (Krutzik and Nolan, 2003). Cells were analyzed on a LSRII flow cytometer (BD Biosciences). Data analysis was done using FlowJo software (Treestar). The antibodies and concentrations are listed in Tables S1-S3. Cell sorting was performed using a FACSAria II (BD Biosciences) cell sorter (SickKids-UHN Flow Cytometry Facility, Toronto). The antibodies and concentrations are listed in Tables S1-S3. For the experiment shown in Fig. 3C,D, the sorted and presort populations were plated on Matrigel-coated 12-well plates at a density of 600,000 cells/well.

Immunohistochemistry

Cells were fixed with 4% paraformaldehyde for 20 min at room temperature, permeabilized in 0.2% Triton X-100 for 20 min at room temperature, and then blocked in PBS+2% BSA+10% secondary antibody-specific serum for 45 min at room temperature. Incubations with primary and secondary antibodies were performed in PBS+0.05% Triton X-100+2% BSA. DAPI was used to stain nuclei. Pictures of immunostained cells were acquired using a Leica CTR6000 fluorescence microscope and the Leica Application Suite software. For co-staining with HDE1 or HDE2, fixed cells were first blocked and stained with HDE1 or HDE2 and secondary antibody in PBS+2% BSA, then permeabilized and stained for intracellular proteins. The antibodies and concentrations are listed in Tables S1-S3.

Real-time PCR analysis

Total RNA was extracted with the RNAqueous-Micro Kit (Ambion) and DNase treated (Ambion). Reverse transcription was performed with 1 µg RNA using Superscript III Reverse Transcriptase (Invitrogen). Quantitative PCR was done in a MasterCycler EP RealPlex (Eppendorf) using QuantiFast SYBR Green PCR Kit (Qiagen). The fetal liver sample was a pool of 63 spontaneously aborted fetuses (22-40 weeks; Clontech; cat. no. 636540, lot no. 7030173). Primer sequences are listed in Table S4. Analysis of expression levels was performed using the ΔC_t method, using *TBP* (TATA binding protein) as the housekeeping gene and the control sample value set to 1.

Tissue sections and cell lines

The frozen sections of fetal pancreas came from a 40-week-old male fetus (Biochain; cat. no. T1244188). The frozen sections of fetal liver originated from a 20-week-old female fetus (Biochain; cat. no. T6244700-1). Cadaveric donor tissues were used as the source of adult pancreas and adult liver sections, and these tissues were obtained through the Oregon Health & Science University tissue donation program. The HPDE6 cells were a gift from Senthil K. Muthuswamy (University Health Network, Toronto). The human primary hepatocytes were purchased from Celsis In Vitro Technologies (lot no. OSI). The liver carcinoma cells HepG2 and Huh7 were a gift from Dr Rebecca R. Laposa (University of Toronto).

Development (2015) 142, 4253-4265 doi:10.1242/dev.121020

Statistical analysis

Statistical analysis was performed using the one-way ANOVA and paired *t*-tests.

Acknowledgements

We thank Maria Grompe, Claire Turina and YongPing Zhong from the Streeter laboratory for their efforts in generating the HDE1 and HDE2 antibodies. We thank members of the Keller laboratory, especially James Surapisitchat, for helpful discussions; Simona Principe and Thomas Kislinger for their efforts in trying to identify the antibody epitopes.

Competing interests

The authors declare no competing or financial interests.

Author contributions

A.H. and G.K. designed experiments and wrote the paper. The laboratory of P.R.S. generated and purified the HDE1 and HDE2 antibodies. S.O. provided technical advice on hepatocyte differentiation. A.H., F.S., S.H. and S.O. carried out the experiments. A.H. analyzed the data. M.N. generated mesodermal cells for the original antibody screens.

Funding

This work was supported by a National Institutes of Health grant [5U01DK089561-05 to G.K.]. A.H. was supported by the McEwen postdoctoral fellowship. Deposited in PMC for release after 12 months.

Supplementary information

Supplementary information available online at
http://dev.biologists.org/lookup/suppl/doi:10.1242/dev.121020/-/DC1

References

Brafman, D. A., Phung, C., Kumar, N. and Willert, K. (2013). Regulation of endodermal differentiation of human embryonic stem cells through integrin-ECM interactions. *Cell Death Differ.* **20**, 369-381.

Chambers, S. M., Fasano, C. A., Papapetrou, E. P., Tomishima, M., Sadelain, M. and Studer, L. (2009). Highly efficient neural conversion of human ES and iPS cells by dual inhibition of SMAD signaling. *Nat. Biotechnol.* **27**, 275-280.

Chen, Y.-F., Tseng, C.-Y., Wang, H.-W., Kuo, H.-C., Yang, V. W. and Lee, O. K. (2012). Rapid generation of mature hepatocyte-like cells from human induced pluripotent stem cells by an efficient three-step protocol. *Hepatology* **55**, 1193-1203.

Cherry, A. B. C. and Daley, G. Q. (2012). Reprogramming cellular identity for regenerative medicine. *Cell* **148**, 1110-1122.

D'Amour, K. A., Agulnick, A. D., Eliazer, S., Kelly, O. G., Kroon, E. and Baetge, E. E. (2005). Efficient differentiation of human embryonic stem cells to definitive endoderm. *Nat. Biotechnol.* **23**, 1534-1541.

Diecke, S., Jung, S. M., Lee, J. and Ju, J. H. (2014). Recent technological updates and clinical applications of induced pluripotent stem cells. *Korean J. Intern. Med.* **29**, 547-557.

Feng, X., Zhang, J., Smuga-Otto, K., Tian, S., Yu, J., Stewart, R. and Thomson, J. A. (2012). Protein kinase C mediated extraembryonic endoderm differentiation of human embryonic stem cells. *Stem Cells* **30**, 461-470.

Fox, I. J., Daley, G. Q., Goldman, S. A., Huard, J., Kamp, T. J. and Trucco, M. (2014). Use of differentiated pluripotent stem cells in replacement therapy for treating disease. *Science* **345**, 1247391.

Gadue, P., Gouon-Evans, V., Cheng, X., Wandzioch, E., Zaret, K. S., Grompe, M., Streeter, P. R. and Keller, G. M. (2009). Generation of monoclonal antibodies specific for cell surface molecules expressed on early mouse endoderm. *Stem Cells* **27**, 2103-2113.

Gouon-Evans, V., Boussemart, L., Gadue, P., Nierhoff, D., Koehler, C. I., Kubo, A., Shafritz, D. A. and Keller, G. (2006). BMP-4 is required for hepatic specification of mouse embryonic stem cell–derived definitive endoderm. *Nat. Biotechnol.* **24**, 1402-1411.

Green, M. D., Chen, A., Nostro, M. C., d'Souza, S. L., Schaniel, C., Lemischka, I. R., Gouon-Evans, V., Keller, G. and Snoeck, H.-W. (2011). Generation of anterior foregut endoderm from human embryonic and induced pluripotent stem cells. *Nat. Biotechnol.* **29**, 267-272.

Holditch, S. J., Terzic, A. and Ikeda, Y. (2014). Concise review: pluripotent stem cell-based regenerative applications for failing beta-cell function. *Stem Cells Transl. Med.* **3**, 653-661.

Holmgren, G., Sjogren, A.-K., Barragan, I., Sabirsh, A., Sartipy, P., Synnergren, J., Bjorquist, P., Ingelman-Sundberg, M., Andersson, T. B. and Edsbagge, J. (2014). Long-term chronic toxicity testing using human pluripotent stem cell-derived hepatocytes. *Drug Metab. Dispos.* **42**, 1401-1406.

Huang, S. X. L., Islam, M. N., O'Neill, J., Hu, Z., Yang, Y.-G., Chen, Y.-W., Mumau, M., Green, M. D., Vunjak-Novakovic, G., Bhattacharya, J. et al. (2014). Efficient generation of lung and airway epithelial cells from human pluripotent stem cells. *Nat. Biotechnol.* **32**, 84-91.

Iwashita, H., Shiraki, N., Sakano, D., Ikegami, T., Shiga, M., Kume, K. and Kume, S. (2013). Secreted cerberus1 as a marker for quantification of definitive endoderm differentiation of the pluripotent stem cells. *PLoS ONE* **8**, e64291.

Jiang, W., Zhang, D., Bursac, N. and Zhang, Y. (2013). wnt3 is a biomarker capable of predicting the definitive endoderm differentiation potential of hESCs. *Stem Cell Rep.* **1**, 46-52.

Kataoka, H., Takakura, N., Nishikawa, S., Tsuchida, K., Kodama, H., Kunisada, T., Risau, W., Kita, T. and Nishikawa, S.-I. (1997). Expressions of PDGF receptor alpha, c-Kit and Flk1 genes clustering in mouse chromosome 5 define distinct subsets of nascent mesodermal cells. *Dev. Growth Differ.* **39**, 729-740.

Kattman, S. J., Witty, A. D., Gagliardi, M., Dubois, N. C., Niapour, M., Hotta, A., Ellis, J. and Keller, G. (2011). Stage-specific optimization of activin/nodal and BMP signaling promotes cardiac differentiation of mouse and human pluripotent stem cell lines. *Cell Stem Cell* **8**, 228-240.

Kennedy, M., D'Souza, S. L., Lynch-Kattman, M., Schwantz, S. and Keller, G. (2007). Development of the hemangioblast defines the onset of hematopoiesis in human ES cell differentiation cultures. *Blood* **109**, 2679-2687.

Kennedy, M., Awong, G., Sturgeon, C. M., Ditadi, A., LaMotte-Mohs, R., Zúñiga-Pflücker, J. C. and Keller, G. (2012). T lymphocyte potential marks the emergence of definitive hematopoietic progenitors in human pluripotent stem cell differentiation cultures. *Cell Rep.* **2**, 1722-1735.

Köhler, G. and Milstein, C. (1975). Continuous cultures of fused cells secreting antibody of predefined specificity. *Nature* **256**, 495-497.

Krutzik, P. O. and Nolan, G. P. (2003). Intracellular phospho-protein staining techniques for flow cytometry: monitoring single cell signaling events. *Cytometry A* **55A**, 61-70.

Leung, A., Nah, S. K., Reid, W., Ebata, A., Koch, C. M., Monti, S., Genereux, J. C., Wiseman, R. L., Wolozin, B., Connors, L. H. et al. (2013). Induced pluripotent stem cell modeling of multisystemic, hereditary transthyretin amyloidosis. *Stem Cell Rep.* **1**, 451-463.

Loh, K. M., Ang, L. T., Zhang, J., Kumar, V., Ang, J., Auyeong, J. Q., Lee, K. L., Choo, S. H., Lim, C. Y. Y., Nichane, M. et al. (2014). Efficient endoderm induction from human pluripotent stem cells by logically directing signals controlling lineage bifurcations. *Cell Stem Cell* **14**, 237-252.

McGrath, K. E., Koniski, A. D., Maltby, K. M., McGann, J. K. and Palis, J. (1999). Embryonic expression and function of the chemokine SDF-1 and its receptor, CXCR4. *Dev. Biol.* **213**, 442-456.

Medine, C. N., Lucendo-Villarin, B., Storck, C., Wang, F., Szkolnicka, D., Khan, F., Pernagallo, S., Black, J. R., Marriage, H. M., Ross, J. A. et al. (2013). Developing high-fidelity hepatotoxicity models from pluripotent stem cells. *Stem Cells Transl. Med.* **2**, 505-509.

Nostro, M. C., Sarangi, F., Ogawa, S., Holtzinger, A., Corneo, B., Li, X., Micallef, S. J., Park, I.-H., Basford, C., Wheeler, M. B. et al. (2011). Stage-specific signaling through TGFbeta family members and WNT regulates patterning and pancreatic specification of human pluripotent stem cells. *Development* **138**, 861-871.

Ogawa, S., Surapisitchat, J., Virtanen, C., Ogawa, M., Niapour, M., Sugamori, K. S., Wang, S., Tamblyn, L., Guillemette, C., Hoffmann, E. et al. (2013). Three-dimensional culture and cAMP signaling promote the maturation of human pluripotent stem cell-derived hepatocytes. *Development* **140**, 3285-3296.

Ogawa, M., Ogawa, S., Bear, C. E., Ahmadi, S., Chin, S., Li, B., Grompe, M., Keller, G., Kamath, B. M. and Ghanekar, A. (2015). Directed differentiation of cholangiocytes from human pluripotent stem cells. *Nat. Biotechnol.* **33**, 853-861.

Ouyang, H., Mou, L.-j., Luk, C., Liu, N., Karaskova, J., Squire, J. and Tsao, M.-S. (2000). Immortal human pancreatic duct epithelial cell lines with near normal genotype and phenotype. *Am. J. Pathol.* **157**, 1623-1631.

Pagliuca, F. W., Millman, J. R., Gürtler, M., Segel, M., Van Dervort, A., Ryu, J. H., Peterson, Q. P., Greiner, D. and Melton, D. A. (2014). Generation of functional human pancreatic beta cells in vitro. *Cell* **159**, 428-439.

Pan, Y., Ouyang, Z., Wong, W. H. and Baker, J. C. (2011). A new FACS approach isolates hESC derived endoderm using transcription factors. *PLoS ONE* **6**, e17536.

Rezania, A., Bruin, J. E., Arora, P., Rubin, A., Batushansky, I., Asadi, A., O'Dwyer, S., Quiskamp, N., Mojibian, M., Albrecht, T. et al. (2014). Reversal of diabetes with insulin-producing cells derived in vitro from human pluripotent stem cells. *Nat. Biotechnol.* **32**, 1121-1133.

Roelandt, P., Dobbels, P., Komuta, M., Corveleyn, A., Emonds, M.-P., Roskams, T., Aerts, R., Monbaliu, D., Libbrecht, L., Laleman, W. et al. (2013). Heterozygous alpha1-antitrypsin Z allele mutation in presumed healthy donor livers used for transplantation. *Eur. J. Gastroenterol. Hepatol.* **25**, 1335-1339.

Sherwood, R. I., Jitianu, C., Cleaver, O., Shaywitz, D. A., Lamenzo, J. O., Chen, A. E., Golub, T. R. and Melton, D. A. (2007). Prospective isolation and global gene expression analysis of definitive and visceral endoderm. *Dev. Biol.* **304**, 541-555.

Si-Tayeb, K., Noto, F. K., Nagaoka, M., Li, J., Battle, M. A., Duris, C., North, P. E., Dalton, S. and Duncan, S. A. (2010). Highly efficient generation of human hepatocyte-like cells from induced pluripotent stem cells. *Hepatology* **51**, 297-305.

Development (2015) 142, 4253-4265 doi:10.1242/dev.121020

Sjogren, A.-K., Liljevald, M., Glinghammar, B., Sagemark, J., Li, X.-Q., Jonebring, A., Cotgreave, I., Brolén, G. and Andersson, T. B. (2014). Critical differences in toxicity mechanisms in induced pluripotent stem cell-derived hepatocytes, hepatic cell lines and primary hepatocytes. *Arch. Toxicol.* **88**, 1427-1437.

Spence, J. R., Mayhew, C. N., Rankin, S. A., Kuhar, M. F., Vallance, J. E., Tolle, K., Hoskins, E. E., Kalinichenko, V. V., Wells, S. I., Zorn, A. M. et al. (2011). Directed differentiation of human pluripotent stem cells into intestinal tissue in vitro. *Nature* **470**, 105-109.

Sun, P., Zhou, X., Farnworth, S. L., Patel, A. H. and Hay, D. C. (2013). Modeling human liver biology using stem cell-derived hepatocytes. *Int. J. Mol. Sci.* **14**, 22011-22021.

Szkolnicka, D., Farnworth, S. L., Lucendo-Villarin, B., Storck, C., Zhou, W., Iredale, J. P., Flint, O. and Hay, D. C. (2014). Accurate prediction of drug-induced liver injury using stem cell-derived populations. *Stem Cells Transl. Med.* **3**, 141-148.

Toivonen, S., Lundin, K., Balboa, D., Ustinov, J., Tamminen, K., Palgi, J., Trokovic, R., Tuuri, T. and Otonkoski, T. (2013a). Activin A and Wnt-dependent specification of human definitive endoderm cells. *Exp. Cell Res.* **319**, 2535-2544.

Toivonen, S., Ojala, M., Hyysalo, A., Ilmarinen, T., Rajala, K., Pekkanen-Mattila, M., Aanismaa, R., Lundin, K., Palgi, J., Weltner, J. et al. (2013b). Comparative analysis of targeted differentiation of human induced pluripotent stem cells (hiPSCs) and human embryonic stem cells reveals variability associated with incomplete transgene silencing in retrovirally derived hiPSC lines. *Stem Cells Transl. Med.* **2**, 83-93.

Trounson, A., Shepard, K. A. and DeWitt, N. D. (2012). Human disease modeling with induced pluripotent stem cells. *Curr. Opin. Genet. Dev.* **22**, 509-516.

Vitale, A. M., Matigian, N. A., Ravishankar, S., Bellette, B., Wood, S. A., Wolvetang, E. J. and Mackay-Sim, A. (2012). Variability in the generation of induced pluripotent stem cells: importance for disease modeling. *Stem Cells Transl. Med.* **1**, 641-650.

Wang, P., Rodriguez, R. T., Wang, J., Ghodasara, A. and Kim, S. K. (2011). Targeting SOX17 in human embryonic stem cells creates unique strategies for isolating and analyzing developing endoderm. *Cell Stem Cell* **8**, 335-346.

Witte, O. N. (1990). Steel locus defines new multipotent growth factor. *Cell* **63**, 5-6.

Zhou, X., Sun, P., Lucendo-Villarin, B., Angus, A. G. N., Szkolnicka, D., Cameron, K., Farnworth, S. L., Patel, A. H. and Hay, D. C. (2014). Modulating innate immunity improves hepatitis C virus infection and replication in stem cell-derived hepatocytes. *Stem Cell Rep.* **3**, 204-214.

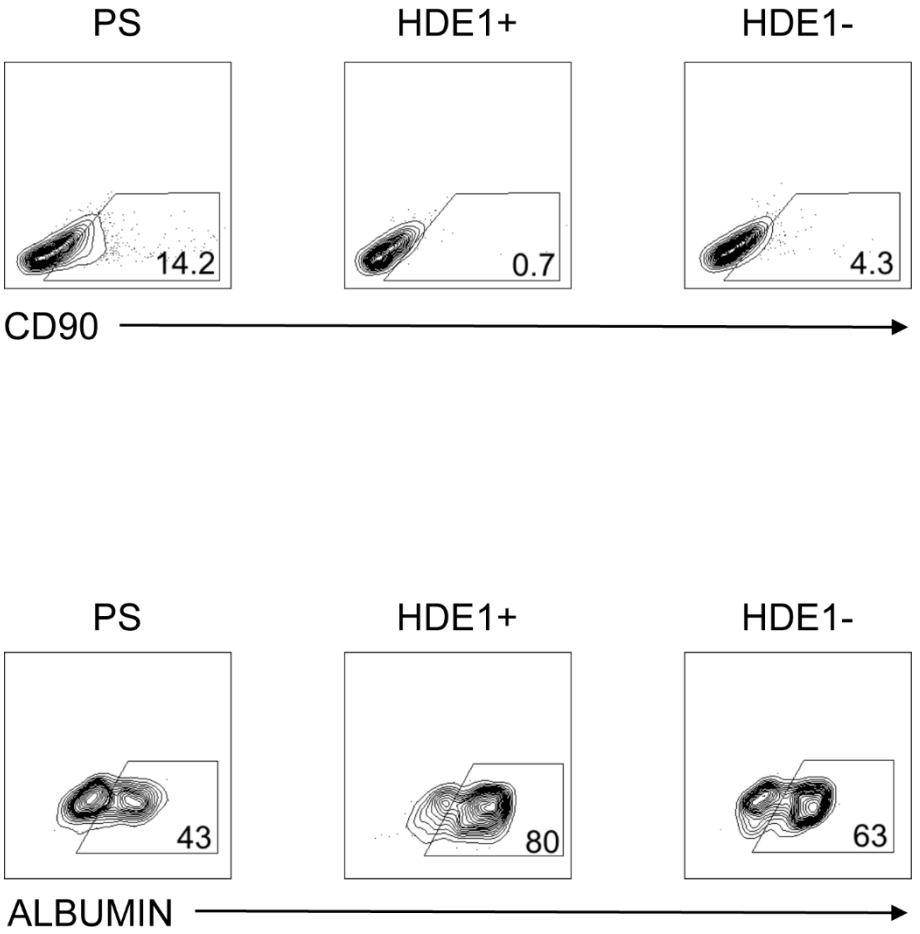

Figure S1. Analysis of the proportion of CD90$^+$ and ALB$^+$ cells in HDE1$^+$ and HDE1$^-$ -derived populations. Representative flow cytometric analyses of CD90 and ALB staining in populations derived from presort (PS), HDE1$^+$ and HDE2$^+$ cells following 28 days of culture as described in figure 3B.

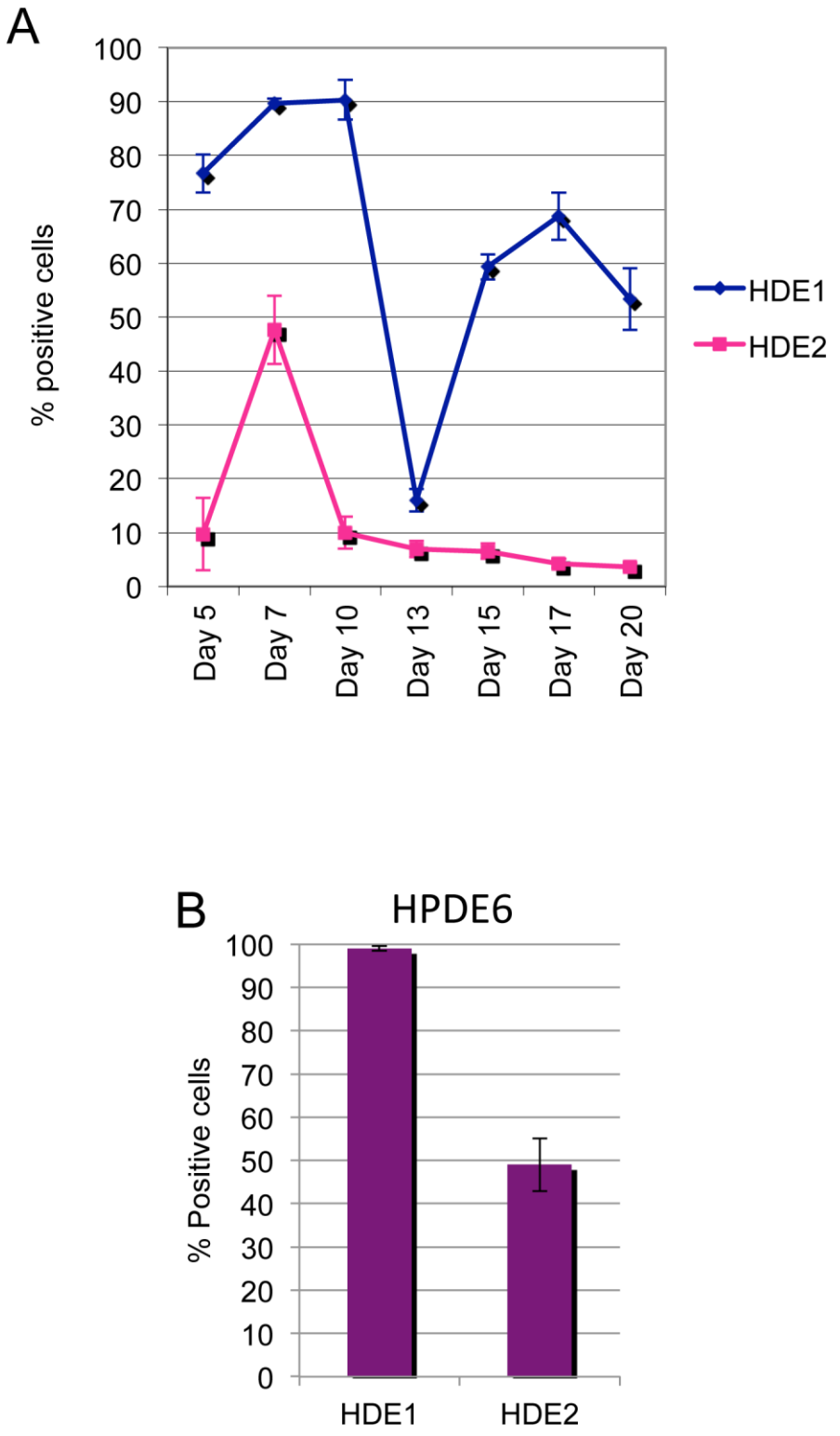

Figure S2. HDE1 and HDE2 staining patterns on hESCs-derived pancreatic populations and on HPDE6 cells. (A) Flow cytometric analyses of HDE1 and HDE2 staining at the indicated time of pancreatic differentiation of HES2 hESCs (n=3, data are represented as mean +/- SEM). (B) Flow cytometric analyses of HDE1 and HDE2 staining of the pancreatic duct epithelial cell line HPDE6 (n=3, data are represented as mean +/- SEM).

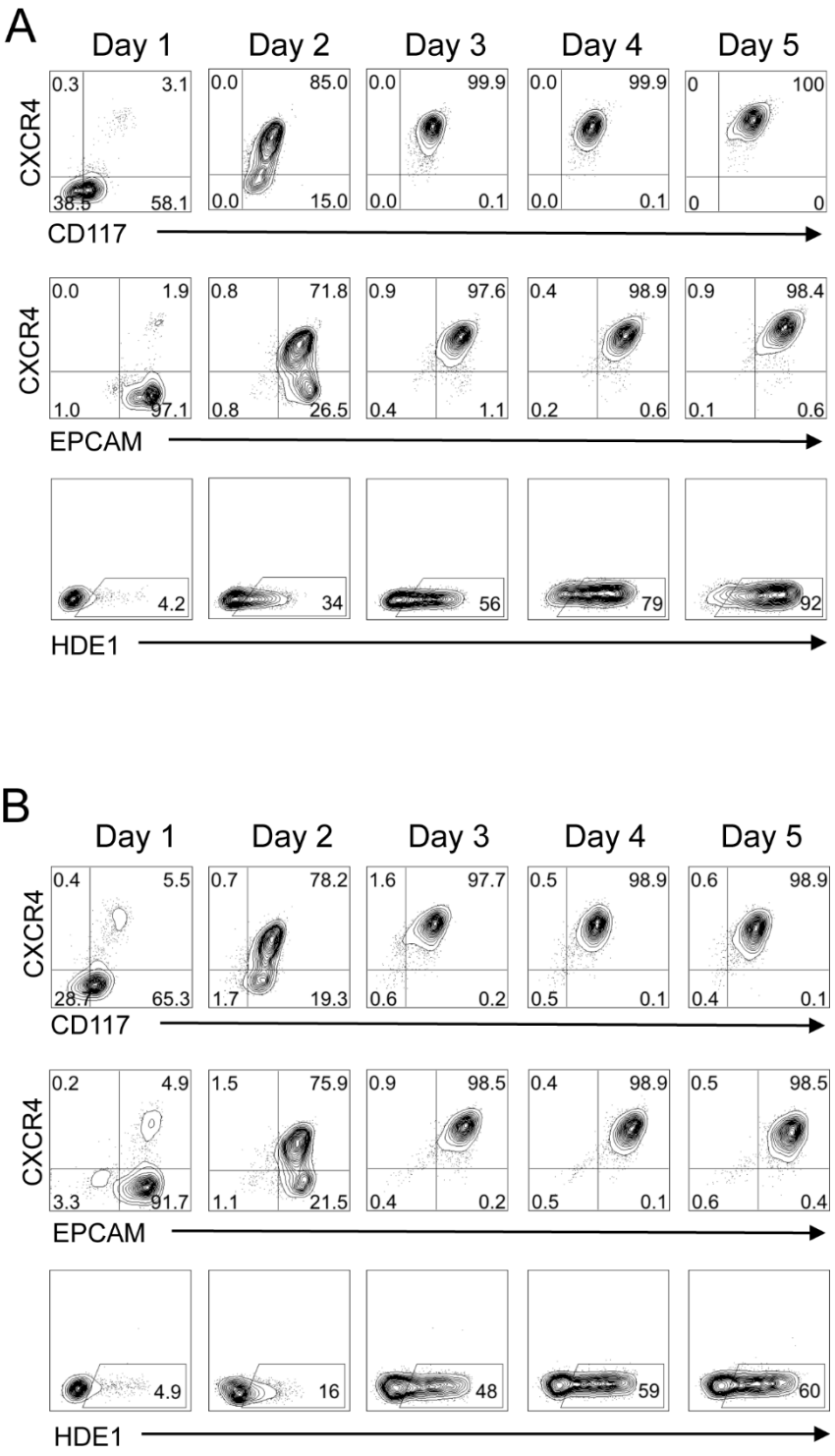

Figure S3. HDE1 and HDE2 staining patterns of definitive endoderm induced in monolayer cultures. (A) Representative flow cytometric analysis of CXCR4, CD117, EPCAM and HDE1 staining of the emerging HES2 hESC-derived endoderm populations induced in monolayer cultures. (B) Representative flow cytometric analysis of CXCR4, CD117, EPCAM and HDE1 staining of the emerging H1 hESC-derived endoderm populations induced in monolayer culture. All FACS plots are representative of the results from 3 independent experiments.

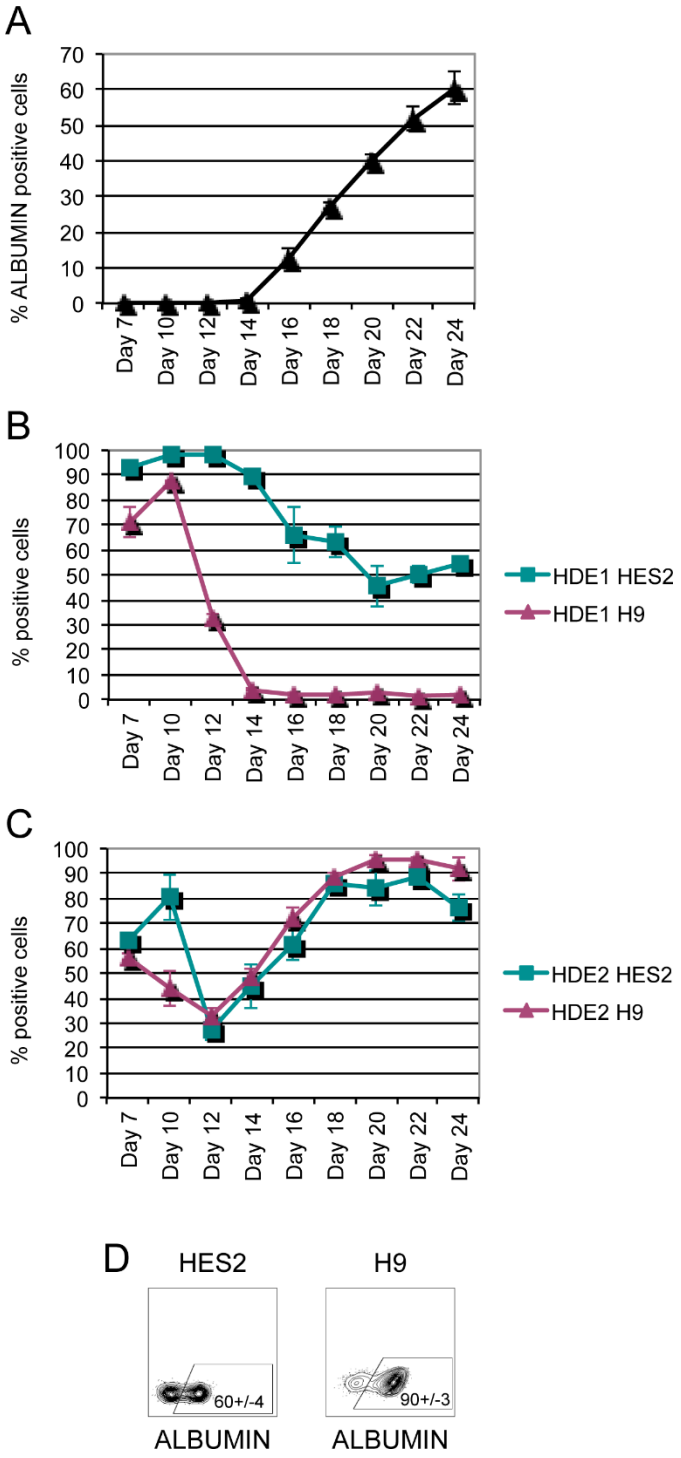

Figure S4. HDE1 and HDE2 staining patterns of HES2 and H9-derived populations at different stages of hepatic development. (A) Intra-cellular flow cytometric analysis of ALB staining at the indicated days of hepatic differentiation of HES2 hESCs (n=3, data are represented as mean +/- SEM). (B) Flow cytometric analysis of HDE1 staining at the indicated days of hepatic differentiation of HES2 and H9 hESCs (n=3, data are represented as mean +/- SEM). (C) Flow cytometric analysis of HDE2 staining at the indicated days of hepatic differentiation of HES2 and H9 hESCs (n=3, data are represented as mean +/- SEM). (D) Percentage of ALB^{+} cells in day 24 hepatocyte cultures generated from either HES2 (left panel) or H9 (right panel) hESCs. Values were determined by intra-cellular flow cytometric analyses (n=3, data are represented as mean +/- SEM)

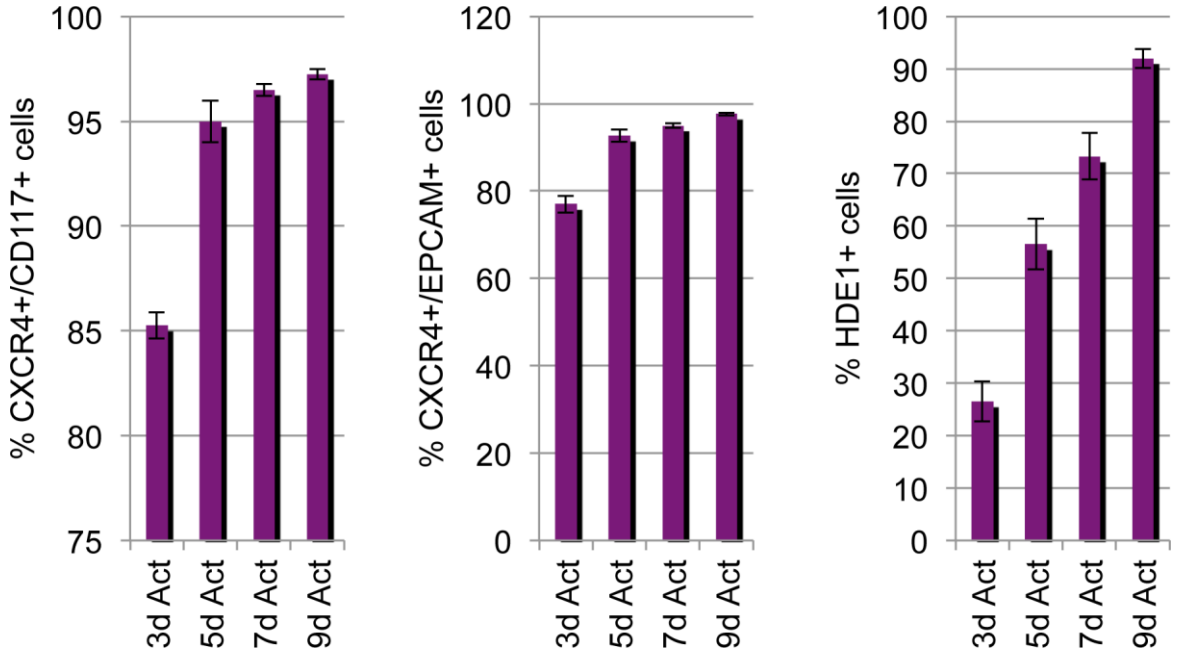

Figure S5. Analyses of H9 hESC-derived endoderm populations induced with activin A for different periods of time. Flow cytometric analysis showing the proportion of $CXCR4^{+}CD117^{+}$ cells, $CXCR4^{+}EPCAM^{+}$ cells and $HDE1^{+}$ cells in H9 hESC-derived populations induced with activin A for the indicated periods of time. (n=3, data are represented as mean +/- SEM).

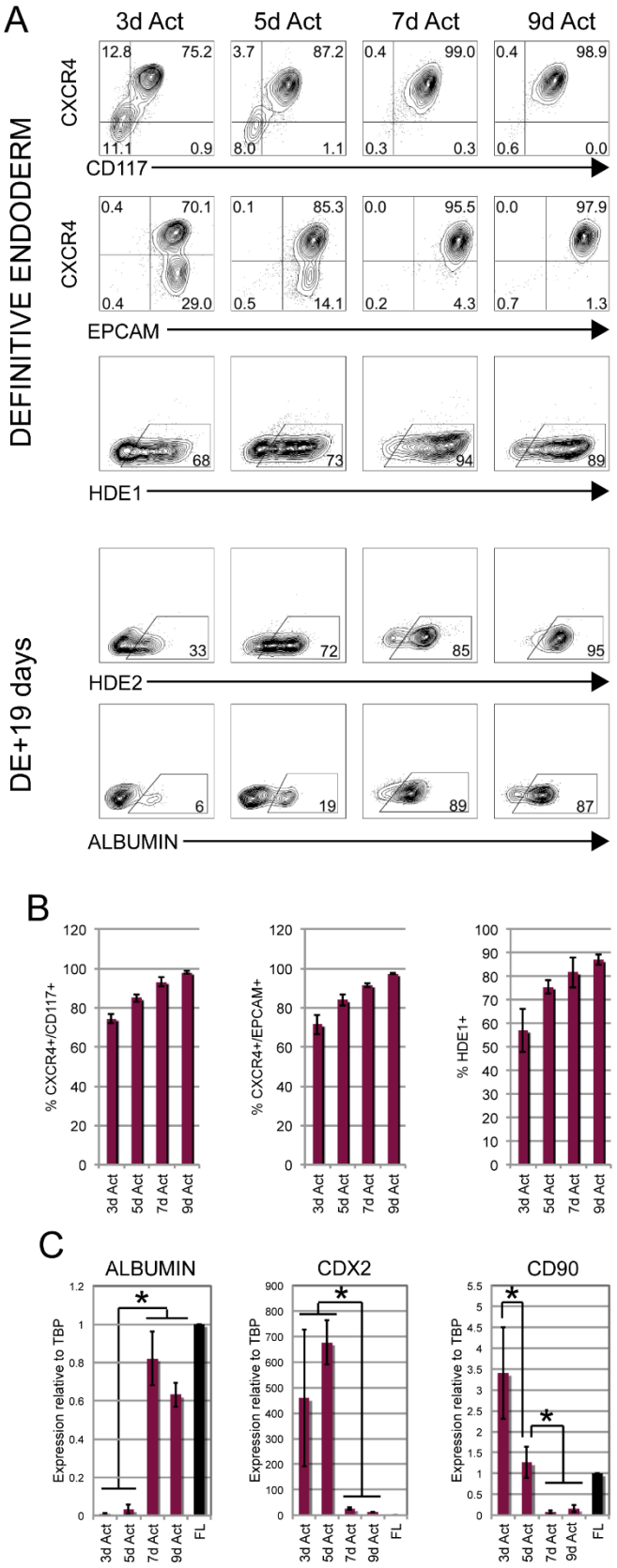

Figure S6. Hepatic potential of BJ hIPSC-derived endoderm correlates with HDE1 staining patterns. (A) Upper three rows: representative flow cytometric analysis showing the proportion of CXCR4$^+$, CD117$^+$ EPCAM$^+$ and HDE1$^+$ cells in BJ hIPSC-derived endoderm populations induced with activin A for the indicated period of time (days). Lower two rows:

representative flow cytometric analysis showing the proportion of $HDE2^+$ and ALB^+ cells in hepatic cultures generated from endoderm induced for the indicated periods of time. Cells were analyzed 19 days following the endoderm stage (DE+19 days). (B) Flow cytometric analysis showing the proportion of $CXCR4^+CD117^+$ cells, $CXCR4^+EPCAM^+$ cells and $HDE1^+$ cells in BJ hIPSC-derived populations induced with activin A for the indicated periods of time. (n=3, data are represented as mean +/- SEM). (C) RT-qPCR analyses of *ALB*, *CDX2* and *CD90* expression in the BJ hIPSC-derived hepatic populations (DE+19) generated from the endoderm induced with activin A for different periods of time. (FL=Fetal Liver). Values were determined relative to TBP and compared to fetal liver (FL set at 1, n=3, data are represented as mean +/- SEM. * indicates $p<0.05$).

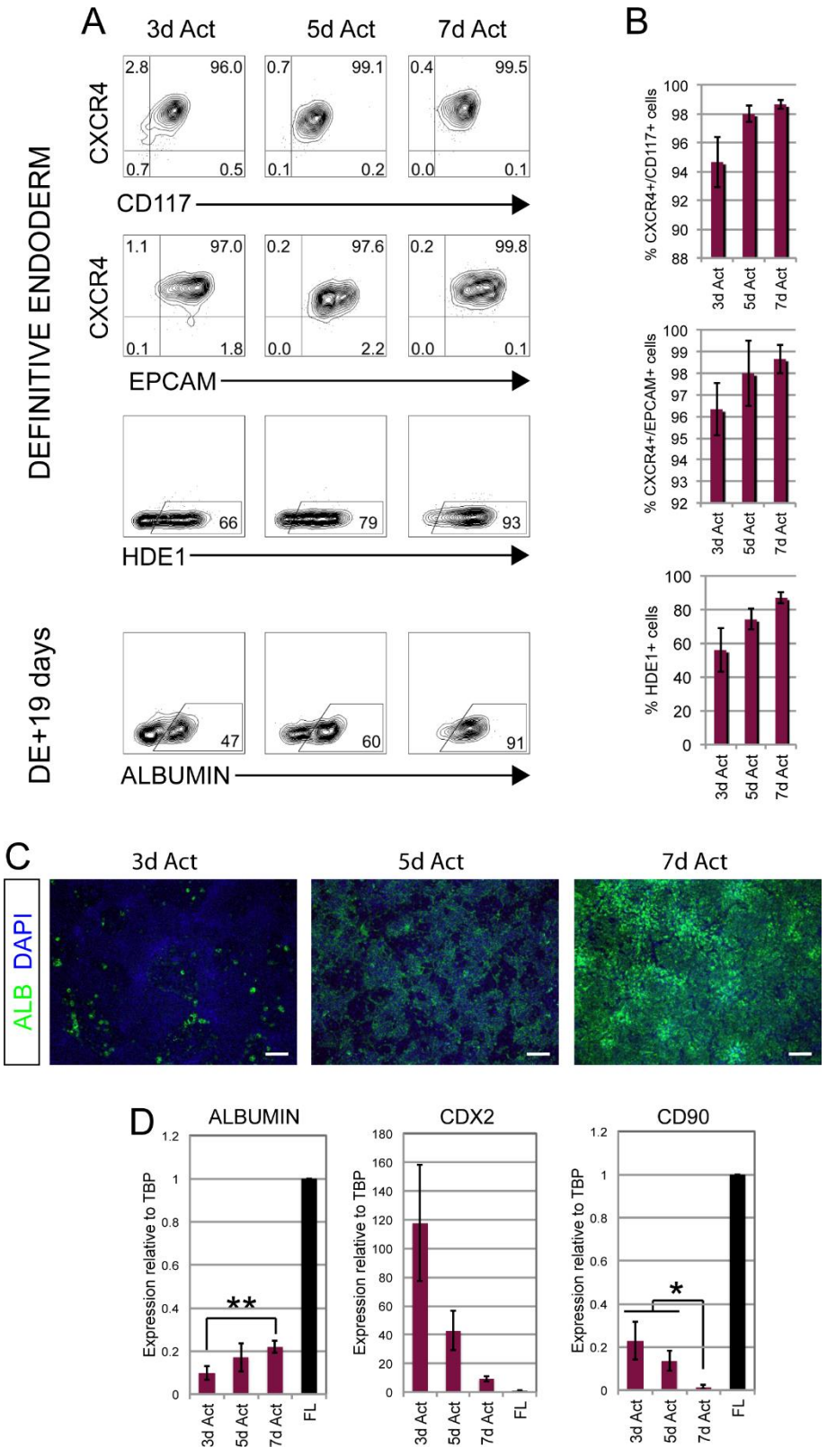

Fig. S7. Hepatic potential of MSC-iPS1 hiPSC-derived endoderm correlates with HDE1 staining patterns. (A) Upper three rows: representative flow cytometric analysis showing the proportion of $CXCR4^+$, $CD117^+$ $EPCAM^+$ and $HDE1^+$ cells in MSC-iPS1 hIPSC-derived endoderm populations induced with activin A for the indicated period of time (days). Lower row: representative flow cytometric analysis showing the proportion of and ALB^+ cells in hepatic cultures generated from endoderm induced for the indicated periods of time. Cells

were analyzed 19 days following the endoderm stage (DE+19 days). (B) Flow cytometric analysis showing the proportion of $CXCR4^{+}CD117^{+}$ cells, $CXCR4^{+}EPCAM^{+}$ cells and $HDE1^{+}$ cells in MSC-iPS1 hIPSC-derived populations induced with activin A for the indicated periods of time. (n=3, data are represented as mean +/- SEM). (C) Immunocytochemistry analyses of ALB (green) expression in MSC-iPS1 hiPSC-derived hepatic populations following 19 days of culture of definitive endoderm stage induced with activin A for the indicated period of time (days). Scale bars: 200 um. (D) RT-qPCR analyses of *ALB*, *CDX2* and *CD90* expression in the MSC-iPS1 hIPSC-derived hepatic populations (DE+19) generated from the endoderm induced with activin A for the indicated periods of time. (FL=Fetal Liver). Values were determined relative to TBP and compared to fetal liver (FL set at 1, n=3, data are represented as mean +/- SEM. * indicates $p<0.05$. ** indicates $p<0.01$).

Table S1. Primary antibody list

Antibody	Company	Catalogue number	Ig Species	Conjugate	Dilution
HDE1	n/a	n/a	Mouse IgG1	none	1:100 (flow and IHC)
HDE2	n/a	n/a	Mouse IgG1	None	1:100 (flow and IHC)
SOX17	R&D	MAB1924	Mouse	None	1:40
CXCR4 (CD184)	BD	555976	Mouse	APC	1:50
CD117	BD	340529	Mouse	PE	1:25
EPCAM (CD326)	eBioscience	12-9326-42	Mouse	PE	1:100
KDR	R&D	FAB357A	Mouse	APC	15:100
KDR	R&D	FAB357P	Mouse	PE	15:100
PDGFRa (CD140a)	BD	556002	Mouse	PE	1:20
CD56	BD	555518	Mouse	APC	1:20
ALBUMIN	Bethyl	A80-129A	Goat	None	1:200 (flow) 1:400 (IHC)
ALBUMIN	DAKO	A0001	Rabbit	None	1:400 (flow) 1:4000 (IHC)
AFP	DAKO	A00008	Rabbit	None	1:2000
CD90	Biolegend	328110	Mouse	PE	1:400
5H10	Streeter lab	n/a	Mouse IgM	None	50ul (supernatant)
HICO 3-C5	Streeter lab	n/a	Mouse IgM	None	50ul (supernatant)
c-peptide	Beta Cell Biology Consortium	AB1921	Rat	None	1:300 (flow) 1:1000 (IHC)

Table S2. IgG control list

Antibody	Company	Catalogue number	Conjugate	Stock concentration
Goat IgG	Sigma	I5256	none	1mg/ml
Rabbit IgG	Jackson Immunoresearch	001-000-003	None	11mg/ml
Mouse IgG1	Life technologies	MG105	APC	4.1mg/ml

Table S3. Secondary antibody list

Antibody	Company	Product Code	Conjugate	Dilution
Goat anti-Mouse IgG	Jackson immunoresearch	115-115-164	PE	1:200
Goat anti-Mouse IgM	Jackson immunoresearch	115-096-075	FITC	1:100
Goat anti-Mouse IgG	Jackson immunoresearch	115-165-164	Cy3	1:200
Donkey anti-Rat IgG	Life technologies	A21208	Alexa488	1:400
Donkey anti-Goat IgG	Life technologies	A11055	Alexa488	1:400
Donkey anti-Rabbit IgG	Life technologies	A11008	Alexa488	1:400
Donkey anti-Rabbit IgG	Jackson immunoresearch	711-165-152	Cy3	1:300

Table S4. RT-qPCR primer list

GENE	Forward sequence	Reverse sequence
ALBUMIN	5'-GTGAAACACAAGCCCAAGGCAACA-3'	5'-TCAGCCTTGCAGCACTTCTCTACA-3'
CD90	5'-ATACCAGCAGTTCACCCATTCAGT-3'	5'-AATTGCTGGTGAAGTTGGTTCGGG-3'
CER	5'-CTTGTCTCAGCTCTGCCACTAACT-3'	5'-TCATCTAGGTCGGGTCCGTCATTT-3'
CXCR4	5'-AGGGAACTGAACATTCCAGAGCGT-3'	5'-AAACGTTCCACGGGAATGGAGAGA-3'
FOXA2	5'-GCATTCCCAATCTTGACACGGTGA-3'	5'-GCCCTTGCAGCCAGAATACACATT-3'
MEOX1	5'-TGAGGACTGATGGCCAAAGAGCAT-3'	5'-ATCCAAACTCACGTTGACCTCCCT-3'
MESP1	5'-AGCCCAAGTGACAAGGGACAACT-3'	5'-AAGGAACCACTTCGAAGGTGCTGA-3'
OCT4	5'-ATGCATTCAAACTGAGGTGCCTGC-3'	5'-CCACCCTTTGTGTTCCCAATTCCT-3'
SOX17	5'-AGGAAATCCTCAGACTCCTGGGTT-3'	5'-CCCAAACTGTTCAAGTGGCAGACA-3'
SOX7	5'-AGCATGCTTCCTTTAGCTGCTGTG-3'	5'-TTGCTCTAAAGCACTGGCTGAGGA-3'
TBP	5′-GCGCAAGGGTTTCTGGTTTGCC-3′	5′-AGGGATTCCGGGAGTCATGGC-3′
ZIC1	5′-GTCTTCGCGCGCTCCGAGAATT-3′	5′-CTTGCGGTCGCTGCTGTTAGCG-3′